Refined stability thresholds for localized spot patterns for the Brusselator model in $\mathbb{R}^2$

Y. Chang*, J. C. Tzou †, M. J. Ward ‡, J. C. Wei §

November 7, 2017

Abstract

In the singular perturbation limit $\epsilon \to 0$, we analyze the linear stability of multi-spot patterns on a bounded 2-D domain, with Neumann boundary conditions, as well as periodic patterns of spots centered at the lattice points of a Bravais lattice in $\mathbb{R}^2$, for the Brusselator reaction-diffusion model

$$v_t = \epsilon^2 \Delta v + \epsilon^2 - v + f u v^2 \,, \qquad \tau u_t = D\Delta u + \frac{1}{\epsilon^2}\left(v - u v^2\right) \,,$$

where the parameters satisfy $0 < f < 1$, $\tau > 0$, and $D > 0$. A previous leading-order linear stability theory characterizing the onset of spot amplitude instabilities for the parameter regime $D = \mathcal{O}(\nu^{-1})$, where $\nu = -1/\log\varepsilon$, based on a rigorous analysis of a nonlocal eigenvalue problem (NLEP), predicts that zero-eigenvalue crossings are degenerate. To unfold this degeneracy, the conventional leading-order-in-ν NLEP linear stability theory for spot amplitude instabilities is extended to one higher order in the logarithmic gauge ν. For a multi-spot pattern on a finite domain under a certain symmetry condition on the spot configuration, or for a periodic pattern of spots centered at the lattice points of a Bravais lattice in $\mathbb{R}^2$, our extended NLEP theory provides explicit and improved analytical predictions for the critical value of the inhibitor diffusivity D at which a competition instability, due to a zero-eigenvalue crossing, will occur. Our higher-order analysis also provides a detailed characterization of the spectrum of the linearization of the spot pattern within the small ball $|\lambda| = \mathcal{O}(\nu) \ll 1$ of the spectral plane whenever D is sufficiently close to this competition stability threshold. For the finite-domain problem the second term in the asymptotic expansion of this critical value of D is shown to depend on the matrix spectrum of the Neumann Green's matrix. For the periodic spot problem, this second term is shown to depend on the regular part of the Bloch Green's function for the Laplacian. Finally, when D is below the competition stability threshold, a different extension of conventional NLEP theory is used to determine an explicit scaling law, with anomalous dependence on ε, for the Hopf bifurcation threshold value of τ that characterizes temporal oscillations in the spot amplitudes.

Key Words: Spot patterns, Brusselator, nonlocal eigenvalue problem, Hopf bifurcation, zero-eigenvalue crossing, competition stability threshold, Bloch Green's function, Bravais lattice.

1 Introduction

Spatially localized 2-D spot patterns are a class of "far-from-equilibrium" [19] patterns that are well-known to occur for certain two-component reaction-diffusion (RD) systems in the singular perturbation limit of a large diffusivity ratio. These localized patterns have been shown to exhibit a wide variety of phenomena such as slow spot dynamics, spot-pinning behavior, spot self-replication, and two types of $\mathcal{O}(1)$ time-scale spot amplitude instabilities that occur in certain parameter regimes (cf. [3], [7], [10], [11], [13], [17], [18], [20], [22], [24], [25], [26], [27], [32], [33], [34], [37]). Localized spot patterns have also been observed in diverse experimental settings [16], [8], and [2]. A survey of localized pattern

*Dept. of Mathematics, University of Washington, Seattle, WA, USA
†Dept. of Mathematics, Macquarie University, Sydney, Australia tzou.justin@gmail.com
‡Dept. of Mathematics, University of British Columbia, Vancouver, BC, Canada (corresponding author ward@math.ubc.ca)
§Dept. of Mathematics, University of British Columbia, Vancouver, BC, Canada jcwei@math.ubc.ca

formation with application to chemical physics is given in [29], while [14] surveys localized pattern formation problems that lead to snaking-type bifurcation diagrams in a range of specific applications. The rich phenomena exhibited by these "far-from-equilibrium" localized patterns has been the impetus for the development of new theoretical tools for their analysis, owing to the fact that conventional Turing-type stability analysis [28] is not applicable. A recent survey of some of these theoretical tools, as applied to the study of localized spot patterns in the Brusselator RD model in 2-D, is given in [30].

In this article we will develop an explicit higher-order asymptotic theory to analyze spot amplitude instabilities for the non-dimensional Brusselator model, formulated in 2-D as

$$v_t = \epsilon^2 \Delta v + \epsilon^2 - v + f u v^2 \,, \qquad \tau u_t = D \Delta u + \frac{1}{\epsilon^2}\left(v - u v^2\right) \,. \tag{1.1}$$

The non-dimensionalization of the original Brusselator model of [21], which leads to (1.1), is given in Appendix A. We will apply our higher-order theory to both periodic patterns of spots in $\mathbb{R}^2$ and to N-spot patterns, with $N \geq 2$, in a bounded 2-D domain with Neumann boundary conditions and under a certain symmetry condition on the configuration of spots involving the Neumann Green's matrix (see (2.7) below).

Mathematically, a spot pattern for (1.1) is a spatial pattern where v is concentrated as $\epsilon \to 0$ near certain discrete spatial points, which then typically drift asymptotically slowly in time towards some steady-state spot configuration (cf. [24], [26]). For these spot patterns, spot amplitude instabilities are $\mathcal{O}(1)$ time-scale instabilities of the spot profile that are fast relative to the asymptotically long time-scale associated with slow spot dynamics, and so these instabilities can be analyzed by "freezing" the spatial configuration $\{\mathbf{x}_1, \ldots, \mathbf{x}_N\}$ of spots. There are two types of spot amplitude instabilities that are associated with locally radially symmetric perturbations of the profiles of the localized spots: competition instabilities due to a zero-eigenvalue crossing, which numerically are found to lead to spot annihilation, and time-periodic oscillatory instabilities of the spot amplitudes resulting from a Hopf bifurcation. One primary challenge for analyzing spot amplitude instabilities in a 2-D setting, that does not occur in the well-studied 1-D case (see [31], [23] and the references therein), is that the key small parameter for the linear stability analysis is the logarithmic gauge $\nu = -1/\log\epsilon$, and that spot amplitude instabilities occur in the parameter regime $D = \mathcal{O}(\nu^{-1})$.

To leading order in ν for the $D = \mathcal{O}(\nu^{-1})$ regime, and with $\tau = \mathcal{O}(1)$, spot amplitude instabilities for the Brusselator (1.1) have been analyzed in [22] from a rigorous spectral analysis of a nonlocal eigenvalue problem (NLEP). This conventional leading-order NLEP theory, as motivated by similar NLEP analyses for other RD systems in [32] and [34] (see also [36]), provides only a leading-order determination of the competition stability threshold in D. Moreover, this leading-order theory also predicts that the zero-eigenvalue crossing is degenerate when $N > 2$, as $N - 1$ distinct spatial modes are predicted to go unstable at the leading-order competition threshold value of D. In addition, with regards to spot amplitude oscillations, the leading-order NLEP theory predicts that there are no oscillatory instabilities of the spot amplitudes for any $\mathcal{O}(1)$ value of τ when D is below this threshold. An open question then is whether a Hopf bifurcation can occur in this regime of D for some $\tau \gg 1$.

In an effort to obtain a higher-order asymptotic theory, a hybrid asymptotic-numerical approach, similar to that first developed in [11] and [7] for other RD systems, was formulated to study spot amplitude instabilities for the Brusselator on the sphere [22] and in a planar 2-D domain [26]. In this formulation, the resulting eigenvalue problem for spot amplitude instabilities is a globally coupled eigenvalue problem (GCEP) that accounts for all powers of ν, but which can only be solved numerically. From this GCEP, quantitatively accurate predictions for the stability thresholds can be computed that result from either zero-eigenvalue crossings or Hopf bifurcations. However, a disadvantage of the GCEP formulation is that analytically it is intractable to track the spectrum of the linearization as parameters are varied, and so no explicit analytical results in the spectral plane are available.

As a compromise between the limitations of the leading-order NLEP theory, and the analytical intractability of the GCEP hybrid asymptotic-numerical eigenvalue formulation, we will develop a higher-order-in-ν extended NLEP theory to analytically calculate certain parameter thresholds for spot amplitude instabilities more accurately than the leading-order NLEP theory. Our higher-order theory, also provides detailed analytical results for the behavior of the spectrum of the linearization near the critical stability thresholds. More specifically, our new focus in this article is to develop a two-term asymptotic theory in the logarithmic gauge ν to both accurately and analytically predict parameter thresholds for instabilities of the amplitudes of a collection of localized spots in the large inhibitor diffusivity regime $D = \mathcal{O}(\nu^{-1})$, where $\nu = -1/\log\varepsilon$. We will consider both N-spot patterns, with $N \geq 2$, in a bounded 2-D domain, under a certain symmetry condition (2.7) on the spatial configuration of spots, as well as a steady-state periodic pattern of spots centered

at the lattice points of a Bravais lattice in $\mathbb{R}^2$. Our higher-order-in-ν linear stability theory for the regime $D = \mathcal{O}(\nu^{-1})$ relies on developing a two-term asymptotic approximation to the eigenvalues of the GCEP, as originally formulated in [22] (see also [26]).

In §2 we briefly outline the hybrid asymptotic-numerical approach of [22] and [26] for constructing quasi-equilibrium spot patterns and for deriving the GCEP governing spot amplitude linear instabilities. Although this analysis, which effectively provides an approximation accurate to all orders in ν, has been given previously, this explicit construction is needed here as a starting point for our new explicit two-term asymptotic analysis in §4–5 below. In §3, we show how a leading-order analysis of the GCEP in the $D = \mathcal{O}(\nu^{-1})$ regime recovers the conventional leading-order NLEP theory, and a rigorous result for the competition instability from this leading-order theory is summarized in Proposition 3.2. In §3.1, for an N-spot pattern on a bounded domain, we derive a modified NLEP to analyze the possibility of spot amplitude temporal oscillations for some $\tau \gg 1$ when D is below the competition stability threshold. From this modified NLEP, we show, for this range of D, that the spot amplitudes will undergo a Hopf bifurcation when $\tau = \tau_H \sim \varepsilon^{-\tau_c}/\nu \gg 1$ for some anomalous threshold $\tau_c > 0$. An explicit formula for τ_c is given in Proposition 3.3.

The main new results from our study are given in §4 and §5. For competition instabilities, which are due to zero-eigenvalue crossings, our explicit two-term asymptotic theory for both the finite-domain and periodic problems in §4 and §5, respectively, will yield a two-term asymptotic expansion for the stability threshold $D_{\text{comp},\varepsilon}$ of the inhibitor diffusivity D in the form $D_{\text{comp},\varepsilon} = D_{0c}/\nu + D_1^\star + o(1)$, for some explicit D_{0c} and $D_1^\star$. However, most importantly, our refined asymptotic theory also provides a detailed characterization of the spectrum of the linearization of the spot pattern within the small ball $|\lambda| = \mathcal{O}(\nu) \ll 1$ of the spectral plane when $D - D_{0c}/\nu = \mathcal{O}(1)$.

For an N-spot pattern on a bounded-domain, in §4 we show that the spectrum for D near the competition threshold is discrete and is determined by the eigenvalues in an $N-1$ dimensional eigenspace of the the Neumann Green's matrix (see Fig. 2 below). Our main spectral result is summarized in Proposition 4.1, and was simply stated without derivation in the survey article [30]. For this bounded domain problem, our explicit two-term theory unfolds the $N-1$ dimensional degeneracy of the zero-eigenvalue crossing inherent with conventional leading-order NLEP theory. Moreover, since the stability threshold is an asymptotic expansion in the logarithmic gauge $\nu = -1/\log\varepsilon$, our two-term theory provides a significantly more accurate and explicit prediction of this threshold than that afforded by leading-order NLEP theory (see Fig. 3 below). This theory also explicitly identifies which spatial mode is the first to lose stability as D is increased.

In contrast, for competition instabilities associated with the periodic spot problem, in §5 we show when $D - D_{0c}/\nu = \mathcal{O}(1)$, for some leading-order threshold D_{0c}, that there is a real-valued continuous band of spectrum within the small ball $|\lambda| = \mathcal{O}(\nu)$ of the spectral plane. This band depends on the regular part $R_{b0}(\boldsymbol{k})$ of the Bloch Green's function for the Laplacian and is parameterized by the Bloch wavevector $\boldsymbol{k}$ (see Fig. 6 below). This main spectral result is given in Proposition 5.1, and it was announced without any derivation in [30]. By detecting the right-most edge of this continuous band, a max-min criterion involving $R_{b0}(\boldsymbol{k})$ is formulated in order to identify that it is a regular hexagonal lattice arrangement of spots that provides an optimal linear stability threshold. A similar methodology to identify optimal periodic lattice arrangements of spots was developed in [10] for the Gierer-Meinhardt, Schnakenberg, and Gray-Scott models. Our extension of this method of [10] to the Brusselator model (1.1) is significantly more intricate as the underlying NLEP has two nonlocal terms, one of which must be eliminated in a self-consistent way.

In §6 we discuss a few open problems for the analysis of spot amplitude instabilities.

Finally, we remark that our higher-order NLEP-type analysis only characterizes spot amplitude instabilities for (1.1) that occur on an $\mathcal{O}(1)$ time-scale when $D = \mathcal{O}(\nu^{-1})$. There are possibly other stability thresholds associated with the small eigenvalues of order $\mathcal{O}(\epsilon^2)$ in the spectrum of the linearization, which are not addressed herein. Unstable eigenvalues of this type correspond to translational perturbations in the spot locations, but are weak instabilities in that they are only realized over asymptotically long $\mathcal{O}(\epsilon^{-2})$ time-scales.

2 Quasi-Equilibrium Spot Patterns and Linear Stability Theory

In this section we briefly outline the asymptotic construction in of a quasi-equilibrium N-spot pattern for (1.1) for a given spot configuration $\{\mathbf{x}_1, \ldots, \mathbf{x}_N\}$, and we derive the globally coupled eigenvalue problem (GCEP) characterizing the linear stability of the quasi-equilibrium pattern to radially symmetric perturbations near the j-th spot.

For $\epsilon \to 0$, we have $v = \mathcal{O}(1)$ in the core of the spot, where $|\mathbf{x} - \mathbf{x}_j| = \mathcal{O}(\epsilon)$, and $v \sim \epsilon^2$ away from the spot centers

where $|\mathbf{x}-\mathbf{x}_j| = \mathcal{O}(1)$. In the core of the j-th spot, we let $u = D^{-1/2}u_j(\rho)$ and $v = D^{1/2}v_j(\rho)$, with $\mathbf{y} = \epsilon^{-1}(\mathbf{x}-\mathbf{x}_j)$ and $\rho \equiv |\mathbf{y}|$, and obtain the radially symmetric core problem (cf. [22])

$$\begin{aligned} &\Delta_\rho v_j - v_j + f u_j v_j^2 = 0\,, \qquad \Delta_\rho u_j + v_j - u_j v_j^2 = 0\,, \qquad \rho \equiv |\mathbf{y}| > 0\,, \\ &u_j'(0) = v_j'(0) = 0\,; \qquad v_j \to 0\,, \qquad u_j \sim S_j \log\rho + \chi(S_j) \quad \text{as} \quad \rho \to \infty\,, \qquad j = 1,\dots,N\,, \end{aligned} \tag{2.1}$$

where $\Delta_\rho \equiv \partial_{\rho\rho} + \rho^{-1}\partial_\rho$. Here the parameter S_j is the source strength for the j-th spot, which will be determined by matching the core solutions to a globally defined outer solution. The function $\chi(S_j)$, which also depends on f, must be determined from a numerical solution to (2.1) by calculating $\lim_{\rho\to\infty}(u_j - S_j\log\rho) = \chi(S_j)$.

To formulate the problem for the global inhibitor field u defined for $|\mathbf{x}-\mathbf{x}_j| \gg \mathcal{O}(\varepsilon)$, we note that the far-field behavior for u_j in (2.1) implies that each spot is represented by a Dirac measure whose strength is proportional to S_j. In this way, in the outer region, (1.1) yields that $v \sim \epsilon^2$, and that the global inhibitor field satisfies

$$D\Delta u = -1 + 2\pi\sqrt{D}\sum_{j=1}^{N} S_j\delta(\mathbf{x}-\mathbf{x}_j)\,, \quad \mathbf{x}\in\Omega\,; \qquad \partial_n u = 0\,, \quad \mathbf{x}\in\partial\Omega\,. \tag{2.2a}$$

Labeling $\nu \equiv -1/\log\epsilon \ll 1$ and $\chi(S_j) \equiv \chi_j$, the asymptotic matching conditions yield that

$$u \sim D^{-1/2}\left(S_j\log|\mathbf{x}-\mathbf{x}_j| + S_j/\nu + \chi_j\right) \quad \text{as} \quad \mathbf{x}\to\mathbf{x}_j\,, \quad j = 1,\dots,N\,. \tag{2.2b}$$

The key feature in (2.2b) is that in each singularity condition $u \sim A_j\log|\mathbf{x}-\mathbf{x}_j| + B_j$, the regular part, B_j, of it is prescribed. This yields one constraint for each $j = 1,\dots,N$. We then solve (2.2) in terms of the Neumann Green's function for any small fixed ν, to obtain a nonlinear algebraic system (NAS) for the spot strengths S_j for $j = 1,\dots,N$. In this way, our construction of quasi-equilibria has the effect of summing all the logarithmic terms in powers of ν.

The solution to (2.2) is

$$u = -2\pi D^{-1/2}\sum_{i=1}^{N} S_i G_0(\mathbf{x};\mathbf{x}_i) + \bar{u}\,, \qquad \text{provided that} \qquad 2\pi\sqrt{D}\sum_{j=1}^{N} S_j = |\Omega|\,, \tag{2.3}$$

where $|\Omega|$ is the area of Ω. Here $\bar{u}$ is an unknown constant, and $G_0(\mathbf{x};\mathbf{x}_0)$ is the Neumann Green's function satisfying

$$\begin{aligned} &\Delta G_0 = \frac{1}{|\Omega|} - \delta(\mathbf{x}-\mathbf{x}_0)\,, \quad \mathbf{x}\in\Omega\,; \qquad \partial_n G_0 = 0\,, \quad \mathbf{x}\in\partial\Omega\,; \\ &\int_\Omega G_0\,d\mathbf{x} = 0\,, \qquad G_0 \sim -\frac{1}{2\pi}\log|\mathbf{x}-\mathbf{x}_0| + R_0(\mathbf{x}_0) + o(1) \quad \text{as} \quad \mathbf{x}\to\mathbf{x}_0\,. \end{aligned} \tag{2.4}$$

By calculating the limiting behavior of u in (2.3) as $\mathbf{x}\to\mathbf{x}_j$, we enforce that its regular part agrees with that in the singularity condition (2.2b). This yields that $S_1,\dots,S_N$ and $\bar{u}$ must satisfy the nonlinear algebraic system

$$S_j + 2\pi\nu\left(S_j R_{0j} + \sum_{\substack{i=1\\ i\neq j}}^{N} S_i G_{0ji}\right) + \nu\chi(S_j) = \nu D^{1/2}\bar{u}\,, \qquad j = 1,\dots,N\,; \qquad \sum_{j=1}^{N} S_j = \frac{|\Omega|}{2\pi\sqrt{D}}\,, \tag{2.5}$$

where we have defined $R_{0j} \equiv R_0(\mathbf{x}_j)$, $G_{0ji} \equiv G_0(\mathbf{x}_j;\mathbf{x}_i)$. By eliminating $\bar{u}$ from (2.5), we obtain a NAS for $\mathbf{S}$:

$$\mathbf{S} + 2\pi\nu\left(\mathcal{I}-\mathcal{E}\right)\mathcal{G}_0\mathbf{S} + \nu\left(\mathcal{I}-\mathcal{E}\right)\boldsymbol{\chi} = \frac{|\Omega|}{2\pi N\sqrt{D}}\,\mathbf{e}\,. \tag{2.6a}$$

Here $(\cdot)^T$ denotes the transpose, $\mathcal{I}$ is the $N\times N$ identity matrix, and we have defined

$$\mathbf{S} \equiv \begin{pmatrix} S_1 \\ \vdots \\ S_N \end{pmatrix}, \quad \boldsymbol{\chi} \equiv \begin{pmatrix} \chi_1 \\ \vdots \\ \chi_N \end{pmatrix}, \quad \mathbf{e} \equiv \begin{pmatrix} 1 \\ \vdots \\ 1 \end{pmatrix}, \quad \mathcal{E} \equiv \frac{1}{N}\,\mathbf{e}\mathbf{e}^T\,, \quad (\mathcal{G})_{0ij} \equiv \begin{cases} R_{0j} & i = j \\ G_0(\mathbf{x}_i;\mathbf{x}_j) & i\neq j \end{cases}, \quad i,j = 1,\dots,N\,. \tag{2.6b}$$

When the NAS (2.6) has a solution $S_1, \ldots, S_N$, the Brusselator (1.1) has an N-spot quasi-equilibrium solution for the given spatial configuration $\{\mathbf{x}_1, \ldots, \mathbf{x}_N\}$ of spots. Since a detailed study of the solvability of the NAS for an arbitrary spot configuration is intractable analytically, we will focus our analysis below on "symmetric" spot patterns for which $\mathbf{e} = (1, \ldots, 1)^T$ is an eigenvector of the Neumann Green's matrix $\mathcal{G}_0$, i.e. that

$$\mathcal{G}_0 \mathbf{e} = \kappa_{01} \mathbf{e}\,, \tag{2.7}$$

for some κ_{01}. For such symmetric spot patterns, the NAS (2.6) admits a common source strength solution with

$$S_j = S_c = \frac{|\Omega|}{2\pi\sqrt{D}N}\,, \quad j = 1, \ldots, N\,. \tag{2.8}$$

A ring-pattern of spots, where the ring is concentric within the unit disk, is a simple example of a symmetric spot pattern.

2.1 Linear Stability of Quasi-Equilibrium Spot Patterns

Next, we derive the globally coupled eigenvalue problem (GCEP) characterizing the linear stability of N-spot quasi-equilibria to locally radially symmetric perturbations of the profile of the spot. There are two types of such $\mathcal{O}(1)$ time-scale "spot amplitude" instabilities. A competition instability, due to a zero-eigenvalue crossing, is a sign-changing linear instability that preserves the average spot amplitude, but which ultimately triggers a nonlinear process through which one or more spots are annihilated. The second type is an oscillatory instability of the spot amplitudes, which occurs via a Hopf bifurcation when a complex conjugate pair of eigenvalues of the linearization crosses the imaginary axis.

We let v_e and u_e denote the quasi-equilibrium pattern, and in (1.1) we introduce the perturbation

$$v = v_e + e^{\lambda t}\phi\,, \qquad u = u_e + e^{\lambda t}\eta\,, \tag{2.9}$$

where $|\phi| \ll 1$ and $\eta \ll 1$, This yields the singularly perturbed eigenvalue problem

$$\epsilon^2 \Delta\phi - \phi + 2f u_e v_e \phi + f v_e^2 \eta = \lambda\phi\,, \quad \mathbf{x} \in \Omega\,, \qquad \partial_n \phi = 0\,, \quad \mathbf{x} \in \partial\Omega\,, \tag{2.10a}$$

$$D\Delta\eta + \frac{1}{\epsilon^2}\left(\phi - 2u_e v_e \phi - v_e^2 \eta\right) = \tau\lambda\eta\,, \quad \mathbf{x} \in \Omega\,, \qquad \partial_n \eta = 0\,, \quad \mathbf{x} \in \partial\Omega\,. \tag{2.10b}$$

Near the j-th spot centered at $\mathbf{x}_j$, we have that $v_e \sim D^{1/2} v_j(\rho)$ and $u_e(\rho) \sim D^{-1/2} u_j(\rho)$, with $\mathbf{y} = \epsilon^{-1}(\mathbf{x} - \mathbf{x}_j)$ and $\rho = |\mathbf{y}|$, where u_j and v_j satisfy the core problem (2.1). In the j-th inner region, we introduce the locally radially symmetric eigenfunction

$$\phi(\mathbf{x}) \sim D\Phi_j(\rho)\,, \qquad \eta(\mathbf{x}) \sim N_j(\rho)\,. \tag{2.11}$$

Then, from (2.10), we obtain the following radially symmetric BVP system on $\rho \geq 0$:

$$\Delta_\rho \Phi_j - \Phi_j + 2f u_j v_j \Phi_j + f v_j^2 N_j = \lambda \Phi_j\,, \qquad \Phi_j \to 0 \quad \text{as} \quad \rho \to \infty\,, \tag{2.12a}$$

$$\Delta_\rho N_j + (1 - 2u_j v_j)\Phi_j - v_j^2 N_j = 0\,, \qquad N_j \sim C_j \log\rho + B_j\,, \quad \text{as} \quad \rho \to \infty\,, \tag{2.12b}$$

where $\Delta_\rho \equiv \partial_{\rho\rho} + \rho^{-1}\partial_\rho$, provided that the following consistency condition holds:

$$\tau\lambda\epsilon^2/D \ll 1\,. \tag{2.13}$$

In (2.12b) we have specified the far-field behavior $N_j = \mathcal{O}(\log\rho)$ as $\rho \to \infty$, as is consistent since $\Delta_\rho N_j \to 0$ for $\rho \gg 1$. As a remark, since (2.12) is linear and homogeneous, we can write

$$B_j = C_j \hat{B}_j(\lambda, S_j)\,, \tag{2.14}$$

where $\hat{B}_j(\lambda, S_j)$ must be computed numerically from (2.12) with the far-field conditions $\partial_\rho N_j \sim 1/\rho$ and $\Phi_j \to 0$ as $\rho \to \infty$.

As similar to the analysis of the quasi-equilibrium pattern, the outer problem for η, as obtained by matching the local behavior for η as $\mathbf{x} \to \mathbf{x}_j$ to the far-field behavior of N_j as $\rho \to \infty$, is

$$\Delta\eta - \frac{\tau\lambda}{D}\eta = 2\pi \sum_{i=1}^{N} C_i \delta(\mathbf{x}-\mathbf{x}_i)\,, \quad \mathbf{x}\in\Omega\,, \qquad \partial_n \eta = 0\,, \quad \mathbf{x}\in\partial\Omega\,, \tag{2.15a}$$

$$\eta \sim C_j \log|\mathbf{x}-\mathbf{x}_j| + \frac{C_j}{\nu} + B_j \quad \text{as} \quad \mathbf{x}\to\mathbf{x}_j\,, \quad j=1,\dots,N\,, \tag{2.15b}$$

where $\nu \equiv -1/\log\epsilon$. Since the regular part of the singularity condition in (2.15b) is prescribed, each such condition introduces a constraint. These constraints will lead to the GCEP. The solution to (2.15) is

$$\eta = -2\pi \sum_{i=1}^{N} C_i G_\lambda(\mathbf{x};\mathbf{x}_i)\,, \tag{2.16}$$

where the eigenvalue-dependent Green's function $G_\lambda(\mathbf{x};\mathbf{x}_i)$ satisfies

$$\begin{aligned} &\Delta G_\lambda - \frac{\tau\lambda}{D} G_\lambda = -\delta(\mathbf{x}-\mathbf{x}_i)\,, \quad \mathbf{x}\in\Omega\,; \qquad \partial_n G_\lambda = 0\,, \quad \mathbf{x}\in\partial\Omega\,; \\ &G_\lambda \sim -\frac{1}{2\pi}\log|\mathbf{x}-\mathbf{x}_i| + R_\lambda(\mathbf{x}_i) + o(1) \quad \text{as} \quad \mathbf{x}\to\mathbf{x}_i\,. \end{aligned} \tag{2.17}$$

By letting $\mathbf{x}\to\mathbf{x}_j$ in (2.16), and then enforcing the singularity conditions in (2.15b), we obtain in matrix form that

$$[I + 2\pi\nu\mathcal{G}_\lambda]\,\mathbf{c} + \nu\mathbf{b} = 0\,, \qquad (\mathcal{G}_\lambda)_{ij} \equiv \begin{cases} R_{\lambda j} & i=j \\ G_\lambda(\mathbf{x}_i;\mathbf{x}_j) & i\neq j \end{cases}\,, \tag{2.18}$$

where $\mathbf{c}\equiv(C_1,\dots,C_N)^T$ and $\mathbf{b}\equiv(B_1,\dots,B_N)^T$. In view of (2.14), the GCEP (2.18) is simply a homogeneous linear system of the form $\mathcal{M}(\lambda)\mathbf{c}=0$ for the vector $\mathbf{c}$ of spot amplitude perturbations. This system has a nontrivial solution at values of λ where $\det\mathcal{M}(\lambda)=0$. Since the perturbation in v has the form

$$v = v_e + D\sum_{j=1}^{N} C_j \Phi_j\left[\epsilon^{-1}|\mathbf{x}-\mathbf{x}_j|\right] e^{\lambda t}\,, \tag{2.19}$$

it follows that any eigenvalue of the GCEP (2.18) in $\mathrm{Re}(\lambda)>0$ corresponds to an instability in the spot amplitudes resulting from a locally radially symmetric eigenfunction.

3 NLEP Theory: Spot Patterns in 2-D when $D = D_0/\nu$

In this section we study the linearized stability problem for the distinguished limit $D=D_0/\nu \gg 1$, where $\nu\equiv -1/\log\varepsilon$. In this regime, the GCEP (2.18) reduces to leading order in ν to a nonlocal eigenvalue problem (NLEP). By analyzing the spectrum of this NLEP we will analyze both competition and oscillatory instabilities on a finite domain.

In our derivation of an NLEP from the GCEP (2.18) for the distinguished limit $D=D_0/\nu\gg 1$, we will assume that the spot pattern is symmetric in the sense that (2.7) holds. When $D=\mathcal{O}(\nu^{-1})$, (2.8) yields that the common spot source strength is $S_c=\mathcal{O}(\nu^{1/2})\ll 1$. As a first step to deriving the NLEP, we need to determine a two-term asymptotic solution to the core problem (2.1) when $S_c=\mathcal{O}(\nu^{1/2})$. The result, which is readily derived from §4.1 of [22], is as follows:

Lemma 3.1 *For $S_j = S_c \sim \nu^{1/2}(S_0+\nu S_1+\cdots)$, a two-term expansion for the solution to the core problem (2.1) is*

$$v_j \sim \nu^{1/2}\left(v_{j0}+\nu v_{j1}+\cdots\right)\,, \qquad u_j \sim \nu^{-1/2}\left(u_{j0}+\nu u_{j1}+\cdots\right)\,, \qquad \chi \sim \nu^{-1/2}\left(\chi_0+\nu\chi_1+\cdots\right)\,, \tag{3.1a}$$

where

$$v_{j0} = \frac{w}{f\chi_0}\,, \qquad v_{j1} = -\frac{\chi_1}{f\chi_0^2}w - \frac{1}{\chi_0^3 f^3}v_{1p}\,, \qquad u_{j0}=\chi_0\,, \qquad u_{j1}=\chi_1+\frac{1}{\chi_0 f^2}u_{1p}\,. \tag{3.1b}$$

Here $b \equiv \int_0^\infty \rho w^2\, d\rho$, and $w(\rho)$ is the unique ground-state solution satisfying

$$\Delta_\rho w - w + w^2 = 0\,, \quad 0 < \rho < \infty\,; \qquad w(0) > 0\,, \quad w'(0) = 0\,; \qquad w \to 0 \quad \textit{as} \quad \rho \to \infty\,. \tag{3.1c}$$

In (3.1b), v_{1p} and u_{1p} are defined uniquely by the linear BVPs

$$\begin{aligned} L_0 v_{1p} = w^2 u_{1p}\,, \qquad \Delta u_{1p} = w^2 - f w\,, \\ v_{1p} \to 0 \qquad \textit{and} \qquad u_{1p} \sim b(1-f)\log\rho + o(1) \quad \textit{as} \quad \rho \to \infty\,, \end{aligned} \tag{3.1d}$$

where the operator L_0 is defined by $L_0 \equiv \Delta_\rho - 1 + 2w$, with $\Delta_\rho \equiv \partial_{\rho\rho} + \rho^{-1}\partial_\rho$. Moreover, χ_0 and χ_1 are defined by

$$\chi_0 = \frac{b(1-f)}{f^2 S_0}\,, \qquad \chi_1 = -\frac{b(1-f)}{f^2}\frac{S_1}{S_0^2} - \frac{S_0}{b^2(1-f)}\int_0^\infty \rho\, v_{1p}\, d\rho\,. \tag{3.1e}$$

To derive the leading-order NLEP, in (2.12) we expand

$$\Phi_j \sim \nu\left(\Phi_{j0} + \nu\Phi_{j1} + \cdots\right), \quad N_j \sim N_{j0} + \nu N_{j1} + \cdots, \quad B_j = B_{j0} + \nu B_{j1} + \cdots, \quad C_j = \nu\left(C_{j0} + \nu C_{j1} + \cdots\right). \tag{3.2}$$

Upon substituting (3.2) into (2.12), and by using (3.1a) for the core solution v_j and u_j, we obtain that

$$\begin{aligned} L_0\Phi_{j0} + \frac{w^2}{f\chi_0^2}N_{j0} = \lambda\Phi_{j0}\,, \qquad \Phi_{j0} \to 0 \quad \text{as} \quad \rho \to \infty\,, \\ \Delta_\rho N_{j0} = 0\,, \qquad N_{j0} \sim B_{j0} \quad \text{as} \quad \rho \to \infty\,, \end{aligned} \tag{3.3}$$

where $L_0\Phi_{j0} \equiv \Delta_\rho\Phi_{j0} - \Phi_{j0} + 2w\Phi_{j0}$. We conclude that $N_{j0} = B_{j0}$. At next order, we obtain that N_{j1} satisfies

$$\Delta_\rho N_{j1} = -\left(1 - \frac{2w}{f}\right)\Phi_{j0} + \frac{w^2}{f^2\chi_0^2}N_{j0}\,, \qquad N_{j1} \sim C_{j0}\log\rho + B_{j1} \quad \text{as} \quad \rho \to \infty\,. \tag{3.4}$$

By using the divergence theorem on (3.4), we conclude that

$$C_{j0} = \frac{b}{f^2\chi_0^2}B_{j0} + \int_0^\infty \rho\left(\frac{2w}{f} - 1\right)\Phi_{j0}\, d\rho\,. \tag{3.5}$$

Next, we integrate the equation for Φ_{j0} in (3.3) to calculate $\int_0^\infty \rho\Phi_{j0}\, d\rho$ as

$$\int_0^\infty \rho\Phi_{j0}\, d\rho = \frac{1}{\lambda+1}\left[2\int_0^\infty \rho w\Phi_{j0}\, d\rho + \frac{b}{f\chi_0^2}B_{j0}\right]. \tag{3.6}$$

This allows us to eliminate $\int_0^\infty \rho\Phi_{j0}\, d\rho$ in (3.5) for C_{j0}. Then, by substituting $C_j = \nu C_{j0} + \cdots$ and $B_j = B_{j0} + \cdots$ into the GCEP (2.18), we obtain in vector form, with $\mathbf{c}_0 \equiv (C_{10}, \ldots, C_{N0})^T$ and $\mathbf{b}_0 \equiv (B_{10}, \ldots, B_{N0})^T$, that

$$(\mathcal{I} + 2\pi\nu\mathcal{G}_\lambda)\mathbf{c}_0 + \mathbf{b}_0 = 0\,. \tag{3.7}$$

Here for self-consistency we must ensure that $\nu\mathcal{G}_\lambda = \mathcal{O}(1)$. This is done below in two distinct parameter regimes. Then, by substituting (3.6) and (3.5) into (3.7), we derive that $\mathbf{b}_0$ satisfies the matrix problem

$$\left[\frac{b}{f\chi_0^2}(\lambda+1-f)\mathcal{I} + f(\lambda+1)\left(\mathcal{I} + 2\pi\nu\mathcal{G}_\lambda\right)^{-1}\right]\mathbf{b}_0 = -2(\lambda+1-f)\int_0^\infty \rho w\boldsymbol{\Phi}_0\, d\rho\,, \tag{3.8}$$

where $\boldsymbol{\Phi}_0 \equiv (\Phi_{10}, \ldots, \Phi_{N0})^T$. We then use (3.1e) for χ_0, together with $S_0 = |\Omega|/(2\pi N\sqrt{D_0})$, to write

$$\frac{f^2\chi_0^2}{b} = D_0\theta\,, \qquad \theta \equiv \frac{4\pi^2 N^2(1-f)^2 b}{f^2|\Omega|^2}\,. \tag{3.9}$$

Upon substituting (3.8) into (3.3) for Φ_{j0} (recalling $N_{j0} = B_{j0}$ for $j = 1, \ldots, N$), and using (3.9), we obtain the vector NLEP

$$L_0\mathbf{\Phi}_0 - \mathcal{K}w^2 \frac{\int_0^\infty \rho w \mathbf{\Phi}_0 \, d\rho}{\int_0^\infty \rho w^2 \, d\rho} = \lambda \mathbf{\Phi}_0 \,, \qquad \mathbf{\Phi}_0 \to 0 \quad \text{as} \quad \rho \to \infty \,, \tag{3.10a}$$

where the matrix $\mathcal{K}$ is defined by

$$\mathcal{K} \equiv 2(\lambda + 1 - f) \left[(\lambda + 1 - f)\mathcal{I} + D_0\theta(\lambda + 1) \left(\mathcal{I} + 2\pi\nu\mathcal{G}_\lambda \right)^{-1} \right]^{-1} . \tag{3.10b}$$

To diagonalize this vector NLEP, we introduce the matrix spectrum of the λ-dependent Green's matrix $\mathcal{G}_\lambda$ as

$$\mathcal{G}_\lambda \mathbf{v}_j = \kappa_j \mathbf{v}_j \,, \quad j = 1, \ldots, N \,. \tag{3.11}$$

In this way, in terms of the matrix eigenvalues κ_j of $\mathcal{G}_\lambda$, (3.10) yields the N scalar NLEPs given by

$$L_0\Psi - \beta_j(\lambda) w^2 \frac{\int_0^\infty w\Psi\rho \, d\rho}{\int_0^\infty w^2 \rho \, d\rho} = \lambda\Psi \,, \qquad \beta_j = \frac{2(\lambda + 1 - f)}{(\lambda + 1)\left[1 + \frac{D_0\theta}{1 + 2\pi\nu\kappa_j}\right] - f} \,, \qquad j = 1, \ldots, N \,, \tag{3.12}$$

where $\Psi \to 0$ as $\rho \to \infty$. Here $D_0 = D\nu$, θ is defined in (3.9), and κ_j depends on λ through the Green's matrix $\mathcal{G}_\lambda$.

The conventional parameter regime for which $\nu\kappa_j = \mathcal{O}(1)$ in (3.12) is where $D = D_0/\nu$ and $\tau = \mathcal{O}(1)$. This regime is studied in this section. The second regime is for $D = D_0/\nu$ but where τ has the anomalous scaling $\tau = \mathcal{O}\left(\epsilon^{-\tau_c}/\nu\right)$ for some $\tau_c > 0$. This second regime is discussed in §3.1 below in the context of oscillatory instabilities in the spot amplitudes.

For the regime where $D = D_0/\nu$ and $\tau = \mathcal{O}(1)$, (2.17) readily yields for $\nu \ll 1$ and $\lambda \neq 0$ that

$$\mathcal{G}_\lambda = \frac{D_0 N}{\nu\tau\lambda|\Omega|}\mathcal{E} + \mathcal{G}_0 + \mathcal{O}(\nu) \,, \qquad \mathcal{E} \equiv \frac{1}{N}\mathbf{e}\mathbf{e}^T \,, \tag{3.13}$$

where $\mathbf{e} \equiv (1, \ldots, 1)^T$. Then, since $\mathcal{E}\mathbf{e} = \mathbf{e}$ and $\mathcal{E}\mathbf{q}_j = 0$ for $j = 2, \ldots, N$ where $\mathbf{q}_j^T\mathbf{e} = 0$, the eigenvalues κ_j of $\mathcal{G}_\lambda$ are $\kappa_1 \sim D_0 N/\left[\nu\tau\lambda|\Omega|\right]$ and $\kappa_j = \mathcal{O}(1)$ for $j = 2, \ldots, N$. In this way, we obtain that

$$2\pi\nu\kappa_1 \sim \frac{\mu}{\tau\lambda} \,; \qquad 2\pi\nu\kappa_j = \mathcal{O}(\nu) \,, \quad \text{for} \quad j = 2, \ldots, N \,, \quad \text{where} \quad \mu \equiv \frac{2\pi N D_0}{|\Omega|} \,. \tag{3.14}$$

The eigenpair κ_1 and $\mathbf{v}_1 = \mathbf{e}$ is referred to as the synchronous mode, while the other $N - 1$ eigenpairs κ_j and $\mathbf{v}_j = \mathbf{q}_j$, with $\mathbf{q}_j^T\mathbf{e} = 0$ for $j = 2, \ldots, N$, are referred to as the asynchronous, or competition, modes. These latter modes preserve the sum of the spot amplitudes owing to the fact that $\mathbf{q}_j^T\mathbf{e} = 0$, for $j = 2, \ldots, N$.

By substituting (3.14) into the NLEP (3.12), we obtain the following two distinct multipliers of the NLEP corresponding to either asynchronous or synchronous perturbations in the spot amplitudes:

$$\beta_a \equiv \frac{2(\lambda + 1 - f)}{(\lambda + 1)(1 + D_0\theta) - f} \,, \quad \beta_s \equiv \frac{2(\lambda + 1 - f)}{(\lambda + 1)h(\tau\lambda) - f} \,, \quad \text{where} \quad h(\tau\lambda) \equiv 1 + \frac{D_0\theta\tau\lambda}{\tau\lambda + \mu} \,, \quad \mu \equiv \frac{2\pi D_0 N}{|\Omega|} \,. \tag{3.15}$$

In [35] and [36], and more recently using a rigorous winding number approach in [27] and applied to the Brusselator in [30], several key rigorous results have been established for the spectrum of NLEPs of the form (3.12) when β_j is a bilinear function of λ. Since β_a in (3.15) is bilinear, these results can readily be used to analyze the linear stability properties for the asynchronous modes. The following result for the competition instability threshold, corresponding to a zero-eigenvalue crossing for the asynchronous modes, was proved in Proposition 3.3 of [30]. We summarize it as follows.

Proposition 3.2 *Let $N \geq 2$, and consider the NLEP (3.12) for the asynchronous modes where $\beta_j = \beta_a$, as given in (3.15). Then, $Re(\lambda) < 0$ if and only if*

$$D < D_{comp} \sim D_{0c}/\nu \,, \qquad D_{0c} \equiv \frac{|\Omega|^2 f^2}{4\pi^2 N^2 b(1 - f)} \,, \quad \textit{where} \quad b \equiv \int_0^\infty \rho w^2 \, d\rho \,. \tag{3.16}$$

When $D > D_{comp}$, the NLEP (3.12) has a unique positive real eigenvalue.

In §4, our new focus will be to extend the NLEP theory to one higher order in ν in order to obtain a two-term asymptotic result for the critical value D_c of D at which a competition stability occurs. Moreover, we will provide a detailed analysis of the spectrum of the linearization near this critical value.

3.1 Hopf Bifurcation for the Synchronous Mode

In this subsection we briefly discuss a few recent results in [30] for oscillatory instabilities of the spot amplitudes resulting from a Hopf bifurcation of the NLEP (3.12) for the synchronous mode where the multiplier β_s is given in (3.15).

Since $\beta_s = 2 + \mathcal{O}(\tau)$ for $\tau \ll 1$, we have from Theorem 3.7 of [35] that $\mathrm{Re}(\lambda) < 0$. This proves that the synchronous mode is linearly stable for all D_0 when $\tau \ll 1$. Next, we observe from (3.15) that $\beta_s = 2$ when $\lambda = 0$, which from (3.12) yields the null-solution $\Psi = 0$ (see Lemma 4.3 below). For the synchronous mode, we conclude that there can never be a zero-eigenvalue crossing for the NLEP (3.12) for any parameter values. These two observations motivate seeking a Hopf bifurcation value of τ where a complex conjugate pair of eigenvalues enter $\mathrm{Re}(\lambda) > 0$ through the imaginary axis as τ is increased.

This Hopf threshold value of τ was computed numerically in §4 of [30] by developing a new parameterization for the NLEP (3.12) for purely complex eigenvalues of the form $\lambda = i\lambda_I$. For $f = 0.5$, a normalized Hopf threshold τ_H/μ and the Hopf eigenvalue λ_{IH} are plotted versus D_0 in the left and right panels of Fig. 1. From Fig. 1(a), we conclude that there is a unique Hopf bifurcation threshold τ_H only on the range $D_0 > D_{0c}$, and that $\tau_H \to +\infty$ and $\lambda_{IH} \to 0^+$ as $D_0 \to D_{0c}^+$. The scaling law for this behavior, as derived in §4 of [30] is

$$\lambda_{IH} \sim \sqrt{\frac{D_0}{D_{0c}} - 1}\left(\frac{1}{(1-f)^2} - 2\kappa_c\right)^{-1/2}, \qquad \tau_H \sim \frac{\mu_0(1-f)}{\left(\frac{D_0}{D_{0c}} - 1\right)}\left(\frac{1}{(1-f)^2} - 2\kappa_c\right), \quad \text{as} \quad D_0 \to D_{0c}^+, \tag{3.17}$$

where $\mu_0 \equiv 2\pi N D_{0c}/|\Omega|$. Here $\kappa_c \equiv \left[\int_0^\infty \rho\,(w + \rho w'/2)^2\, d\rho\right] / \int_0^\infty \rho w^2\, d\rho \approx 0.436$.

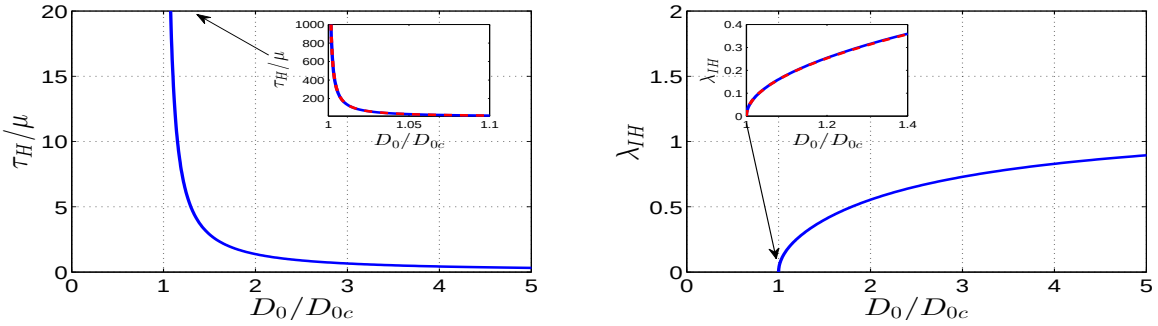

(a) τ_H/μ versus D_0/D_{0c} (b) λ_{IH} versus D_0/D_{0c}

Figure 1: From [30]: The Hopf bifurcation threshold τ_H/μ (left panel) and Hopf eigenvalue λ_{IH} (right panel) versus D_0/D_{0c} when $f = 0.5$ for the synchronous mode of instability for the NLEP (3.12) with multiplier β_s in (3.15). There is no Hopf threshold for $D_0/D_{0c} < 1$, and $\tau_H \to +\infty$ while $\lambda_{IH} \to 0^+$ as $D_0/D_{0c} \to 1^+$. The inserts validate the scaling law of (3.17) (dashed curves) as $D_0/D_{0c} \to 1^+$.

Together with the result in Proposition 3.2 for the competition modes, we conclude for $\nu \ll 1$ that the synchronous mode is linearly stable when $D < D_{0c}/\nu$ for any $\tau > 0$ with $\tau = \mathcal{O}(1)$. When $D > D_{0c}/\nu$, there is always a unique positive real eigenvalue of the NLEP for the competition modes, in addition to an unstable complex conjugate pair of eigenvalues for the synchronous mode when τ increases above the Hopf bifurcation threshold τ_H.

Since the scaling law (3.17) yields that $\tau_H \lambda_{IH}/D \to \infty$ as $D \to D_{0c}/\nu$ for the synchronous mode, the assumption that $|\tau\lambda/D| \ll 1$, which was used in (3.13) to derive the NLEP with the multiplier β_s in (3.15), is not valid as $D \to D_{0c}/\nu$. In [30] (see also [27] for related RD systems) this was the motivation for considering a new asymptotic limit for the range $\tau \gg 1$, but that still ensures that $\nu\kappa_j = \mathcal{O}(1)$, as required in (3.12). Assuming that $|\tau\lambda/D| \gg 1$, we obtain that the eigenvalue-dependent Green's function G_λ in (2.17) is well-approximated by the free space Green's function $G_{f,\lambda}$, so that

$$G_\lambda(\mathbf{x};\mathbf{x}_0) \sim G_{f,\lambda}(\mathbf{x};\mathbf{x}_0) \equiv \frac{1}{2\pi} K_0\left(\theta_\lambda|\mathbf{x} - \mathbf{x}_0|\right), \qquad \theta_\lambda \equiv \sqrt{\tau\lambda\nu/D_0}\,. \tag{3.18}$$

Here the principal branch of the square root is specified to ensure that $G_{f,\lambda}(\mathbf{x};\mathbf{x}_0)$ decays exponentially away from $\mathbf{x}_0$. Since $K_0(z)$ has exponential decay as $|z| \to \infty$ in $\mathrm{Re}(z) > 0$, we obtain for $|\theta_\lambda| \gg 1$ that the Green's matrix $\mathcal{G}_\lambda$ is,

asymptotically proportional to the identity, and is given by $\mathcal{G}_\lambda \sim R_{f,\lambda}\mathcal{I}$ where $R_{f,\lambda}$ is the regular part of $G_{f,\lambda}$. This regular part is readily calculated by using the asymptotics of $K_0(z)$ for $z \to 0^+$. Therefore, in (3.12) and (3.11), we get in terms of Euler's constant γ_e that

$$2\pi\nu\kappa_j \sim 2\pi\nu R_{f,\lambda} = \nu\left(-\frac{1}{2}\log(\nu\tau\lambda) + \log\left(2\sqrt{D_0}\right) - \gamma_e\right). \tag{3.19}$$

The key observation from (3.19) is that $2\pi\nu\kappa_j = \mathcal{O}(1)$, when τ is chosen to have an anomalous scaling of the form

$$\tau \equiv \epsilon^{-\tau_c}/\nu\,, \tag{3.20}$$

where $\tau_c > 0$ is an $\mathcal{O}(1)$ parameter. With this scaling, (3.19) reduces to

$$2\pi\nu\kappa_j = -\frac{\tau_c}{2} + \nu\mathcal{K}_0\,, \qquad \mathcal{K}_0 \equiv -\frac{1}{2}\log\lambda + \log\left(2\sqrt{D_0}\right) - \gamma_e\,. \tag{3.21}$$

By substituting (3.21) into (3.12) we obtain a modified NLEP problem in which τ_c is a parameter. By analyzing this modified NLEP, a Hopf bifurcation threshold value of $\tau_c > 0$ was identified in [30]. From (3.20) this yields a Hopf bifurcation threshold with $\tau_H \gg 1$ in the regime where $D < D_{0c}/\nu$. This result of [30] is summarized as follows:

Proposition 3.3 *For an N-spot pattern for the Brusselator (1.1) when $D = D_0/\nu$ and $D_0 < D_{0c}$, where D_{0c} is the competition instability threshold defined in (3.16), the NLEP (3.12) has a Hopf bifurcation, corresponding to temporal oscillations in the spot amplitudes, when $\tau = \tau_H$ and $\lambda = \pm i\lambda_I$, where*

$$\begin{aligned} &\tau_H \sim \frac{1}{\nu}\epsilon^{-\tau_c}\,, \quad \tau_c = 2\left(1 - \frac{D_0}{D_{0c}}\right) - \nu\log\nu + \nu\left(2\log\left(2\sqrt{D_0}\right) - 2\gamma_e - \log\lambda_{I0}\right) + \mathcal{O}(\nu^2)\,, \\ &\lambda \sim i\nu\lambda_{I0} + \mathcal{O}(\nu^3)\,, \qquad \lambda_{I0} \equiv \frac{\pi D_{0c}}{4D_0}(1-f)\,. \end{aligned} \tag{3.22}$$

We remark that for $\nu \ll 1$, we have $0 < \tau_c < 2$, since $D_0 < D_{0c}$. Thus, with $\lambda = \mathcal{O}(\nu)$ it follows that our required consistency condition (2.13) is satisfied. We further remark that this anomalous Hopf threshold is not uniformly valid in the limit $D_0 \to D_{0c}^+$ for which $\tau_c \to 0^+$. In the narrow regime where $D_0 - D_{0c}$ is asymptotically small, the Hopf bifurcation threshold must be computed numerically from (3.12) by using the eigenvalues κ_j of $\mathcal{G}_\lambda$. We do not pursue this here.

4 Refined Asymptotic Analysis of the Competition Stability Threshold

A key observation in the analysis leading to Proposition 3.2 is that the leading-order competition stability threshold $D \sim D_{0c}/\nu$ for $\nu \ll 1$ occurs as a result of a zero-eigenvalue crossing for an $N-1$ dimensional subspace of asynchronous perturbations in the spot amplitudes, as characterized by $\mathbf{q}_j^T\mathbf{e} = 0$ for $j = 2,\dots,N$. In this sense, this leading order competition stability threshold is degenerate, and a higher-order asymptotic analysis is required to unfold this zero-eigenvalue crossing, and to determine a more refined prediction of the competition instability threshold. More specifically, we now introduce the de-tuning parameter D_1 by

$$D = D_{0c}/\nu + D_1 + o(1)\,, \tag{4.1}$$

so that by expanding $S = \nu^{1/2}(S_0 + \nu S_1 + \cdots)$ as in Lemma 3.1, we obtain from (2.8) that

$$S_0 = \frac{|\Omega|}{2\pi N\sqrt{D_{0c}}}\,, \qquad S_1 = -\frac{D_1}{2D_{0c}}S_0\,. \tag{4.2}$$

Our goal is to determine the eigenvalues λ in the spectrum of the linearization within a small ball $|\lambda| = \mathcal{O}(\nu) \ll 1$ near the origin that are associated with asynchronous perturbations in the spot amplitudes. This detailed analysis is a new result for spot patterns in a finite domain. It was simply stated, without derivation, in the survey article [30] as follows:

Proposition 4.1 *Let $\nu \ll 1$, $N \geq 2$, $\tau = \mathcal{O}(1)$, and suppose that the symmetry condition (2.7) on the spot configuration $\{\mathbf{x}_1, \ldots, \mathbf{x}_N\}$ holds. Then, for $D = D_{0c}/\nu + D_1 + o(1)$, the spectrum of the NLEP corresponding to asynchronous perturbations in the spot amplitudes has discrete eigenvalues λ near the origin, with $|\lambda| = \mathcal{O}(\nu) \ll 1$, given by*

$$\lambda = 2\nu(1-f)\left[-\pi\kappa_{0j} + \frac{D_1}{2D_{0c}} + \frac{1}{2b^2(1-f)}\int_0^\infty \rho v_{1p}\, d\rho\right] + o(\nu)\,, \tag{4.3a}$$

where v_{1p} is defined in (3.1d). Here κ_{0j}, for $j = 2, \ldots, N$, are the eigenvalues of the Neumann Green's matrix $\mathcal{G}_0$ in the $N-1$ dimensional subspace orthogonal to $\mathbf{e}$, i.e.

$$\mathcal{G}_0\mathbf{q}_j = \kappa_{0j}\mathbf{q}_j\,, \quad j = 2, \ldots, N\,, \qquad \text{where} \qquad \mathbf{q}_j^T\mathbf{e} = 0\,. \tag{4.3b}$$

A schematic plot of the spectrum near the origin is shown in Fig. 2. To determine the stability threshold, we simply determine the largest discrete eigenvalue $\lambda_{\rm edge}$ from (4.3a), which is given in terms of the smallest κ_{0j}, and then choose a small enough de-tuning parameter D_1 to ensure that $\lambda_{\rm edge} < 0$. This yields the following result:

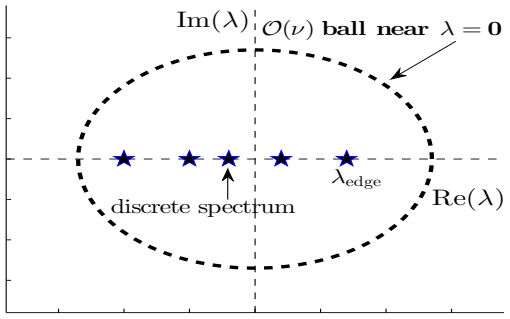

Figure 2: Discrete real eigenvalues within the small ball $|\lambda| = \mathcal{O}(\nu)$ for the case where the Green's matrix $\mathcal{G}_0$ has five distinct eigenvalues κ_{0j} in the subspace orthogonal to $\mathbf{e}$. The de-tuning parameter D_1 is chosen small enough to ensure that the largest such eigenvalue λ_{edge} satisfies $\lambda_{edge} < 0$.

Corollary 4.2 *Let $\nu \ll 1$, $N \geq 2$, then there is a zero-eigenvalue crossing for the asynchronous modes at the (possibly) $N-1$ distinct values of D, given by*

$$D \sim D_{j\epsilon} \equiv \frac{D_{0c}}{\nu}\left[1 + \nu\left(2\pi\kappa_{0j} - \frac{1}{b^2(1-f)}\int_0^\infty \rho v_{1p}\, d\rho\right)\right]\,, \quad j = 2, \ldots, N\,, \tag{4.4}$$

where v_{1p} is defined in (3.1d). The competition instability threshold, defined by $D_{comp,\varepsilon} = \min_j D_{j\epsilon}$, is

$$D_{comp,\varepsilon} \sim \frac{D_{0c}}{\nu}\left[1 + \nu\left(2\pi\kappa_{min} - \frac{1}{b^2(1-f)}\int_0^\infty \rho v_{1p}\, d\rho\right)\right]\,, \qquad \kappa_{min} \equiv \min_{j\in\{2,\ldots,N\}} \kappa_{0j}\,. \tag{4.5}$$

For the asynchronous modes, we have $Re(\lambda) < 0$ when $D < D_{comp,\varepsilon}$.

The rest of this section is devoted to a derivation of our main result in Proposition 4.1. For D near the competition threshold, we introduce the de-tuning of the diffusivity D in (4.1) and consider the neighborhood near $\lambda = 0$,

$$\lambda = \nu\lambda_1 + o(\nu)\,. \tag{4.6}$$

Then, upon writing the N inner problems in (3.3) in vector form with $\mathbf{\Phi}_0 = (\Phi_{10}, \ldots, \Phi_{N0})^T$, $\mathbf{N}_0 = (N_{10}, \ldots, N_{N0})^T$, and $\mathbf{b}_0 = (B_{10}, \ldots, B_{N0})^T$, we obtain with $\lambda = \mathcal{O}(\nu)$ that

$$L_0\mathbf{\Phi}_0 + \frac{w^2}{f\chi_0^2}\mathbf{N}_0 = 0\,, \quad \mathbf{\Phi}_0 \to 0 \quad \text{as} \quad \rho \to \infty\,; \qquad \Delta_\rho\mathbf{N}_0 = 0\,, \quad \mathbf{N}_0 \sim \mathbf{b}_0 \quad \text{as} \quad \rho \to \infty\,. \tag{4.7}$$

Since $L_0 w = w^2$, we conclude from (4.7) that

$$\mathbf{\Phi}_0 = -\frac{w}{f\chi_0^2}\mathbf{b}_0\,, \qquad \mathbf{b}_0 = \mathbf{N}_0\,. \tag{4.8}$$

By writing (3.4) in vector form, and expanding $\mathbf{c}$ and $\mathbf{b}$ as (see (3.2))

$$\mathbf{c} = \nu\mathbf{c}_0 + \nu^2\mathbf{c}_1 + \nu^3\mathbf{c}_2 + \cdots\,, \qquad \mathbf{b} = \mathbf{b}_0 + \nu\mathbf{b}_1 + \cdots\,, \tag{4.9}$$

we get

$$\Delta_\rho \mathbf{N}_1 = -\left(1 - \frac{2w}{f}\right)\mathbf{\Phi}_0 + \frac{w^2}{f^2\chi_0^2}\mathbf{N}_0\,, \quad \rho \geq 0\,; \qquad \mathbf{N}_1 \sim \mathbf{c}_0 \log\rho + \mathbf{b}_1 \quad \text{as} \quad \rho \to \infty\,. \tag{4.10a}$$

From the divergence theorem we conclude that

$$\mathbf{c}_0 = \frac{b}{f^2\chi_0^2}\mathbf{b}_0 + \int_0^\infty \rho\left(\frac{2w}{f} - 1\right)\mathbf{\Phi}_0\, d\rho\,. \tag{4.10b}$$

Then, we use (4.8) for $\mathbf{\Phi}_0$ and $\mathbf{N}_0$ in (4.10a), to obtain that

$$\Delta_\rho \mathbf{N}_1 = -\frac{\mathbf{b}_0}{f^2\chi_0^2}\left(w^2 - fw\right)\,, \quad \rho \geq 0\,; \qquad \mathbf{N}_1 \sim \mathbf{c}_0 \log\rho + \mathbf{b}_1 \quad \text{as} \quad \rho \to \infty\,. \tag{4.11a}$$

Upon using $\int_0^\infty \rho w\, d\rho = \int_0^\infty \rho w^2\, d\rho = b$, together with (4.8) for $\mathbf{\Phi}_0$, we calculate $\mathbf{c}_0$ in (4.10b) as

$$\mathbf{c}_0 = \frac{\mathbf{b}_0 b}{f^2\chi_0^2} + \frac{\mathbf{b}_0}{f\chi_0^2}\int_0^\infty \rho\left(1 - \frac{2w}{f}\right) w\, d\rho = \frac{\mathbf{b}_0}{f^2\chi_0^2}\left(b + f\int_0^\infty \rho w\, d\rho - 2\int_0^\infty \rho w^2\, d\rho\right) = \frac{b}{f^2\chi_0^2}\,(f-1)\,\mathbf{b}_0\,. \tag{4.11b}$$

Next, we set $\lambda \sim \nu\lambda_1$ and $D = \nu^{-1}\left(D_{0c} + \nu D_1 + \nu^2 D_2 + \cdots\right)$ in (3.13) and in the GCEP of (2.18) to obtain

$$\left(\mathcal{I} + \frac{2\pi N}{\tau\nu\lambda_1|\Omega|}\left[D_{0c} + \nu D_1 + \nu^2 D_2 + \cdots\right]\mathcal{E} + 2\pi\nu\mathcal{G}_0\right)\mathbf{c} + \nu\mathbf{b} = 0\,,$$

which can be written as

$$\left(\frac{\mu_0}{\tau\lambda_1}\left(1 + \nu\frac{D_1}{D_{0c}} + \nu^2\frac{D_2}{D_{0c}} + \cdots\right)\mathcal{E} + \nu\mathcal{I} + 2\pi\nu^2\mathcal{G}_0\right)\mathbf{c} = -\nu^2\mathbf{b}\,; \qquad \mu_0 \equiv \frac{2\pi N D_{0c}}{|\Omega|}\,, \quad \mathcal{E} \equiv \frac{1}{N}\mathbf{e}\mathbf{e}^T\,, \tag{4.12}$$

where $\mathcal{G}_0$ is the Neumann Green's matrix.

Upon substituting (4.9) into (4.12), and equating powers of ν, we get

$$\mu_0\mathcal{E}\mathbf{c}_0 = 0\,, \tag{4.13a}$$

$$\mu_0\mathcal{E}\mathbf{c}_1 = \mathcal{R}_1 \equiv -\tau\lambda_1\left(\mathbf{c}_0 + \mathbf{b}_0\right)\,, \tag{4.13b}$$

$$\mu_0\mathcal{E}\mathbf{c}_2 = \mathcal{R}_2 \equiv -\tau\lambda_1\left(\mathbf{c}_1 + \mathbf{b}_1 + 2\pi\mathcal{G}_0\mathbf{c}_0\right) - \mu_0\frac{D_2}{D_{0c}}\mathcal{E}\mathbf{c}_1\,. \tag{4.13c}$$

From (4.13a), and (4.11b), we conclude that $\mathbf{c}_0$, and hence $\mathbf{b}_0$, must lie in the $N-1$ dimensional subspace orthogonal to $\mathbf{e}$. The solvability condition for (4.13b), given by $\tilde{\mathbf{q}}_j^T\mathcal{R}_1 = 0$ for $j = 2, \ldots, N$, for a set of mutually orthogonal vectors $\tilde{\mathbf{q}}_2, \ldots, \tilde{\mathbf{q}}_N$ with $\tilde{\mathbf{q}}_j^T\mathbf{e} = 0$ for $j = 2, \ldots, N$, then enforces that $\mathbf{c}_0 + \mathbf{b}_0 = \mathbf{0}$. In view of (4.11b), we conclude that

$$\mathbf{c}_0 = -\mathbf{b}_0\,, \qquad \mathbf{e}^T\mathbf{c}_0 = 0\,, \qquad \mathbf{e}^T\mathbf{b}_0 = 0\,, \qquad \chi_0 = \frac{\sqrt{b(1-f)}}{f}\,, \qquad \mathbf{c}_1^T\mathbf{e} = 0\,, \tag{4.14}$$

so that $\mathbf{c}_1$ is also orthogonal to $\mathbf{e}$ since $\mathcal{E}\mathbf{c}_1 = \mathbf{0}$. Then, by using (3.1e) for χ_0, together with (4.2), we conclude that

$$S_0 = \frac{\sqrt{b(1-f)}}{f}\,, \qquad D_{0c} = \frac{|\Omega|^2 f^2}{4\pi^2 N^2 b(1-f)}\,, \qquad \text{where} \quad b \equiv \int_0^\infty \rho w\, d\rho\,. \tag{4.15}$$

This reproduces the leading-order competition threshold given in (3.16) of Proposition 3.2.

Next, we substitute $f^2\chi_0^2 = b(1-f)$ into (4.11), to obtain that the problem for $\mathbf{N}_1$ reduces to

$$\Delta_\rho \mathbf{N}_1 = -\frac{\mathbf{b}_0}{b(1-f)}\left(w^2 - fw\right), \quad \rho \geq 0\,; \qquad \mathbf{N}_1 \sim -\mathbf{b}_0 \log\rho + \mathbf{b}_1 \quad \text{as} \quad \rho \to \infty\,. \tag{4.16}$$

Upon comparing (4.16) with the problem (3.1d) for the correction u_{1p} to the core problem as written in Lemma 3.1, we conclude that

$$\mathbf{N}_1 = -\frac{\mathbf{b}_0}{b(1-f)}u_{1p} + \mathbf{b}_1\,. \tag{4.17}$$

To derive the perturbed NLEP problem, which will determine λ_1 via a solvability condition, we must formulate the problems for $\mathbf{N}_2$ and $\mathbf{\Phi}_1$ in the expansion

$$\mathbf{N} = \mathbf{N}_0 + \nu\mathbf{N}_1 + \nu^2\mathbf{N}_2 + \cdots, \qquad \mathbf{\Phi} = \nu\left(\mathbf{\Phi}_0 + \nu\mathbf{\Phi}_1 + \cdots\right). \tag{4.18}$$

By substituting (4.18), together with the expansion (3.1a) for the core solution, into (2.12), and then collecting powers of ν^2 in the equation for N_j, we obtain on $\rho \geq 0$ that

$$\Delta_\rho N_{j2} = -\left(1 - \frac{2w}{f}\right)\Phi_{j1} + 2\left(v_{j1}u_{j0} + v_{j0}u_{j1}\right)\Phi_{j0} + v_{j0}^2 N_{j1} + 2v_{j0}v_{j1}N_{j0}\,. \tag{4.19}$$

We then use (3.1b) for u_{j0}, u_{j1}, v_{j0}, and v_{j1} in (4.19) to obtain in vector form that

$$\begin{aligned}\Delta\mathbf{N}_2 = &-\left(1-\frac{2w}{f}\right)\mathbf{\Phi}_1 + 2\left(\chi_0\left(-\frac{\chi_1 w}{f\chi_0^2} - \frac{v_{1p}}{f^3\chi_0^3}\right) + \frac{w}{f\chi_0}\left(\chi_1 + \frac{u_{1p}}{f^2\chi_0}\right)\right)\mathbf{\Phi}_0 \\ &+ \frac{w^2}{f^2\chi_0^2}\mathbf{N}_1 - \frac{2w}{f\chi_0}\left(\frac{\chi_1 w}{f\chi_0^2} + \frac{v_{1p}}{f^3\chi_0^3}\right)\mathbf{N}_0\,.\end{aligned} \tag{4.20}$$

Then, we substitute $\mathbf{\Phi}_0$ and $\mathbf{N}_0$, as given in (4.8), together with (4.17) for $\mathbf{N}_1$, into (4.20), and recall that $\chi_0^2 f^2 = b(1-f)$. After some algebra, we get that (4.20) reduces to

$$\begin{aligned}&\Delta\mathbf{N}_2 = -\left(1-\frac{2w}{f}\right)\mathbf{\Phi}_1 - \frac{3w^2 u_{1p}}{b^2(1-f)^2}\mathbf{b}_0 - \frac{2w^2 f\chi_1}{[b(1-f)]^{3/2}}\mathbf{b}_0 + \frac{w^2}{b(1-f)}\mathbf{b}_1\,, \quad \rho \geq 0\,, \\ &\mathbf{N}_2 \sim \mathbf{c}_1\log\rho + \mathbf{b}_2\,, \quad \text{as} \quad \rho \to \infty\,.\end{aligned} \tag{4.21}$$

Upon using the divergence theorem on (4.21), and using $b = \int_0^\infty \rho w^2\,d\rho$, we can calculate $\mathbf{c}_1$ as

$$\mathbf{c}_1 = \int_0^\infty \rho\left(\frac{2w}{f} - 1\right)\mathbf{\Phi}_1\,d\rho + \frac{\mathbf{b}_1}{(1-f)} - \frac{3\mathbf{b}_0}{b^2(1-f)^2}\int_0^\infty \rho w^2 u_{1p}\,d\rho - \frac{2f\chi_1 b}{[b(1-f)]^{3/2}}\mathbf{b}_0\,. \tag{4.22}$$

Next, we derive the problem for Φ_{j1}. By substituting (4.18), together with (3.1a) for the expansion of the core solution, into the equation for Φ_j in (2.12), we obtain from the $\mathcal{O}(\nu)$ terms that

$$L_0\Phi_{j1} + 2f\left(v_{j1}u_{j0} + v_{j0}u_{j1}\right)\Phi_{j0} + 2fN_{j0}v_{j0}v_{j1} + \frac{w^2}{f\chi_0^2}N_{j1} = \lambda_1\Phi_{j0}\,, \tag{4.23}$$

on $\rho \geq 0$. We then use (3.1b) for u_{j0}, u_{j1}, v_{j0}, and v_{j1} in (4.23), together with $\mathbf{\Phi}_0$, $\mathbf{N}_0$, and $\mathbf{N}_1$ as given in (4.8) and (4.17). In this way, and recalling that $\chi_0^2 f^2 = b(1-f)$, we obtain after some algebra that (4.23) reduces to

$$L_0\mathbf{\Phi}_1 - \frac{3w^2 f u_{1p}}{b^2(1-f)^2}\mathbf{b}_0 + \frac{w^2 f}{b(1-f)}\mathbf{b}_1 - \frac{2w^2 f^2\chi_1}{[b(1-f)]^{3/2}}\mathbf{b}_0 = -\frac{\lambda_1 f w}{b(1-f)}\mathbf{b}_0\,, \qquad \rho \geq 0\,, \tag{4.24}$$

where $\mathbf{\Phi}_1 \to \mathbf{0}$ as $\rho \to \infty$, and $L_0\mathbf{\Phi}_1 \equiv \Delta_\rho\mathbf{\Phi}_1 - \mathbf{\Phi}_1 + 2w\mathbf{\Phi}_1$.

In order to obtain a perturbed NLEP with only one, rather than two, nonlocal terms we need to isolate $\int_0^\infty \rho\mathbf{\Phi}_1\,d\rho$. To do so, we integrate (4.24) over $0<\rho<\infty$, to obtain

$$-\int_0^\infty \rho\mathbf{\Phi}_1\,d\rho = -\int_0^\infty 2\rho w\mathbf{\Phi}_1\,d\rho + \frac{3f\mathbf{b}_0}{b^2(1-f)^2}\int_0^\infty \rho w^2 u_{1p}\,d\rho - \frac{f}{(1-f)}\mathbf{b}_1 + \frac{2bf^2\chi_1}{[b(1-f)]^{3/2}}\mathbf{b}_0 - \frac{\lambda_1 f}{1-f}\mathbf{b}_0\,. \tag{4.25}$$

We then use (4.25) in (4.22) to eliminate $\int_0^\infty \rho\mathbf{\Phi}_1\,d\rho$. This yields that

$$\mathbf{c}_1 = \frac{(1-f)}{f}\int_0^\infty 2\rho w\mathbf{\Phi}_1\,d\rho + \mathbf{b}_1 - \frac{3\mathbf{b}_0}{b^2(1-f)}\int_0^\infty \rho w^2 u_{1p}\,d\rho - \frac{2\chi_1 f}{[b(1-f)]^{1/2}}\mathbf{b}_0 - \frac{\lambda_1 f}{1-f}\mathbf{b}_0\,. \tag{4.26}$$

A further relation between $\mathbf{c}_1$, $\mathbf{b}_0$, and $\mathbf{b}_1$ is obtained by imposing a solvability condition on the second-order correction term in (4.13c). Since $\mathcal{E}\mathbf{c}_1 = 0$ and $\mathbf{c}_0 = -\mathbf{b}_0$ from (4.14), this solvability condition is that

$$\tilde{\mathbf{q}}_j^T\left(\mathbf{c}_1 + \mathbf{b}_1 - 2\pi\mathcal{G}_0\mathbf{b}_0\right) = 0\,, \quad j = 2,\ldots,N\,, \qquad \tilde{\mathbf{q}}_j^T\mathbf{e} = 0\,, \quad j = 2,\ldots,N\,, \tag{4.27}$$

for any such set of mutually orthogonal vectors $\tilde{\mathbf{q}}_2,\ldots\tilde{\mathbf{q}}_N$.

To analyze (4.27) we first recall from (4.14) that $\mathbf{e}^T\mathbf{b}_0 = 0$ and $\mathbf{e}^T\mathbf{c}_1 = 0$ so that $\mathbf{c}_1$ and $\mathbf{b}_0$ must lie in the $N-1$ dimensional subspace orthogonal to $\mathbf{e}$. Moreover, since $\mathcal{G}_0$ is a symmetric matrix, and under our assumption that the spot configuration $\{\mathbf{x}_1,\ldots,\mathbf{x}_N\}$ is symmetric in the sense that (2.7) holds, we must have that

$$\mathcal{G}_0\mathbf{q}_j = \kappa_{0j}\mathbf{q}_j\,, \qquad j = 2,\ldots,N\,; \qquad \mathbf{e}^T\mathbf{q}_j = 0\,, \quad j = 2,\ldots,N\,, \qquad \mathbf{q}_j^T\mathbf{q}_k = 0\,, \quad j\neq k\,, \tag{4.28}$$

for some mutually orthogonal set $\mathbf{q}_1,\ldots,\mathbf{q}_N$. As such, we conclude that $\mathcal{G}_0\mathbf{b}_0$ is orthogonal to $\mathbf{e}$. In terms of these eigenvectors of $\mathcal{G}_0$, we define the $N-1$ dimensional subspace $\mathcal{Q}^\perp$, together with its orthogonal complement $\mathcal{Q}^\parallel$, by

$$\mathcal{Q}^\perp \equiv \text{span}\{\mathbf{q}_2,\ldots,\mathbf{q}_N\}\,, \qquad \mathcal{Q}^\parallel \equiv \text{span}\{\mathbf{e}\}\,, \qquad \text{where} \qquad \mathbf{e}\equiv(1,\ldots,1)^T\,. \tag{4.29}$$

We then decompose $\mathbf{b}_1$ and $\mathbf{\Phi}_1$ as

$$\mathbf{b}_1 = \mathbf{b}_1^\perp + \mathbf{b}_1^\parallel\,, \qquad \mathbf{\Phi}_1 = \mathbf{\Phi}_1^\perp + \mathbf{\Phi}_1^\parallel\,, \tag{4.30}$$

where $\mathbf{b}_1^\perp\in\mathcal{Q}^\perp$, $\mathbf{b}_1^\parallel\in\mathcal{Q}^\parallel$, $\mathbf{\Phi}_1^\perp\in\mathcal{Q}^\perp$, and $\mathbf{\Phi}_1^\parallel\in\mathcal{Q}^\parallel$. The following Lemma shows $\mathbf{b}_1^\parallel$ and $\mathbf{\Phi}_1^\parallel$ must vanish identically.

Lemma 4.3 *In the decomposition (4.30) we must have* $\mathbf{b}_1^\parallel = 0$ *and* $\mathbf{\Phi}_1^\parallel = 0$. *Therefore,* $\mathbf{e}^T\mathbf{b}_1 = 0$ *and* $\mathbf{e}^T\mathbf{\Phi}_1 = 0$.

Proof: The solvability condition (4.27) provides no constraint on $\mathbf{b}_1^\parallel$. However, from the component of (4.26) in $\mathcal{Q}^\parallel$ we obtain that

$$\mathbf{b}_1^\parallel = -\frac{(1-f)}{f}\int_0^\infty 2\rho w\mathbf{\Phi}_1^\parallel\,d\rho\,. \tag{4.31}$$

By substituting this relation into (4.24), and considering only its component in $\mathcal{Q}^\parallel$, we obtain that $\mathbf{\Phi}_1^\parallel \equiv \mathbf{\Phi}_1^\parallel(\rho)$ satisfies

$$L_0\mathbf{\Phi}_1^\parallel - 2w^2\frac{\int_0^\infty \rho w\mathbf{\Phi}_1^\parallel\,d\rho}{\int_0^\infty \rho w^2\,d\rho} = 0\,, \quad \rho\geq 0\,; \qquad \mathbf{\Phi}_1^\parallel\to 0 \quad \text{as} \quad \rho\to\infty\,, \tag{4.32}$$

which is equivalent to

$$\mathbf{\Phi}_1^\parallel = 2\left(L_0^{-1}w^2\right)\frac{J}{\int_0^\infty \rho w^2\,d\rho}\,, \qquad \text{where} \qquad J\equiv\int_0^\infty \rho w\mathbf{\Phi}_1^\parallel\,d\rho\,.$$

Upon multiplying both sides of this expression by ρw and integrating, and then using the identity $L_0^{-1}w^2 = w$, we get

$$J = \frac{\int_0^\infty 2\rho w\left(L_0^{-1}w^2\right)\,d\rho}{\int_0^\infty \rho w^2\,d\rho}J = 2J\,,$$

which yields $J = \int_0^\infty \rho w\mathbf{\Phi}_1^\parallel\,d\rho = 0$. Since the nonlocal term in (4.32) vanishes, we conclude that $\mathbf{\Phi}_1^\parallel = \mathbf{0}$ since zero is not in the spectrum of L_0 within the class of radially symmetric functions (see [35]). Finally, (4.31), yields that $\mathbf{b}_1^\parallel = \mathbf{0}$. ■

This lemma shows that we need only consider the components of $\mathbf{b}_1$ and $\mathbf{\Phi}_1$ in the subspace $\mathcal{Q}^\perp$, which is orthogonal to $\mathbf{e}$, and is spanned by the eigenvectors of $\mathcal{G}_0$. In this subspace, we obtain from the solvability condition (4.27) that $\mathbf{c}_1 = -\mathbf{b}_1^\perp + 2\pi\mathcal{G}_0\mathbf{b}_0$. Upon substituting this expression into (4.26), and then solving for $\mathbf{b}_1^\perp$, we get

$$\mathbf{b}_1^\perp = \pi\mathcal{G}_0\mathbf{b}_0 - \frac{(1-f)}{f}\int_0^\infty \rho w \mathbf{\Phi}_1^\perp\, d\rho + \frac{3\mathbf{b}_0}{2b^2(1-f)}\int_0^\infty \rho w^2 u_{1p}\, d\rho + \left(\frac{\chi_1 f}{[b(1-f)]^{1/2}} + \frac{\lambda_1 f}{2(1-f)}\right)\mathbf{b}_0\,. \tag{4.33}$$

Finally, we use (4.33) to eliminate $\mathbf{b}_1$ in the component of (4.24) in $\mathcal{Q}^\perp$. After some algebra, and recalling $\sqrt{b(1-f)} = \chi_0 f$, we obtain the following perturbed NLEP problem defined in $\mathcal{Q}^\perp$:

$$\begin{aligned} L_0\mathbf{\Phi}_1^\perp - w^2\frac{\int_0^\infty \rho w \mathbf{\Phi}_1^\perp\, d\rho}{\int_0^\infty \rho w^2\, d\rho} = &-\frac{f}{b(1-f)}\left[\lambda_1\left(w + \frac{fw^2}{2(1-f)}\right) + \pi w^2\mathcal{G}_0\right]\mathbf{b}_0 + \frac{3fw^2u_{1p}}{b^2(1-f)^2}\mathbf{b}_0 \\ &+ w^2\left(\frac{\chi_1}{\chi_0} - \frac{3}{2b^2(1-f)}\int_0^\infty \rho w^2 u_{1p}\, d\rho\right)\frac{f}{b(1-f)}\mathbf{b}_0\,. \end{aligned} \tag{4.34}$$

To diagonalize (4.34), we have for any $\mathbf{b}_0 \in \mathcal{Q}^\perp$ that

$$\mathbf{b}_0 = \sum_{j=2}^N d_j \mathbf{q}_j\,, \tag{4.35}$$

for some coefficients $d_2, \ldots, d_N$. Then, upon decomposing $\mathbf{\Phi}_1^\perp$ as

$$\mathbf{\Phi}_1^\perp = \sum_{j=2}^N \hat{\Phi}_j(\rho)\mathbf{q}_j\,, \tag{4.36}$$

it follows that (4.34) reduces to the $N-1$ scalar perturbed NLEPs

$$\mathcal{L}_0\hat{\Phi}_j \equiv L_0\hat{\Phi}_j - w^2\frac{\int_0^\infty \rho w\hat{\Phi}_j\, d\rho}{\int_0^\infty \rho w^2\, d\rho} = \mathcal{F}_j\,, \qquad \hat{\Phi}_j \to 0 \quad \text{as} \quad \rho\to\infty\,, \tag{4.37a}$$

$$\mathcal{F}_j \equiv -\frac{f\,d_j}{b(1-f)}\left[\lambda_1\left(w + \frac{fw^2}{2(1-f)}\right) + \pi w^2\kappa_{0j} - \frac{3w^2u_{1p}}{b(1-f)} - w^2\left(\frac{\chi_1}{\chi_0} - \frac{3}{2b^2(1-f)}\int_0^\infty \rho w^2 u_{1p}\, d\rho\right)\right]\,, \tag{4.37b}$$

where κ_{0j}, for $j = 2, \ldots, N$, are the eigenvalues of $\mathcal{G}_0$ in the eigenspace $\mathcal{Q}^\perp$ (see (4.28)).

The next step in the calculation is to impose a solvability condition on (4.37) for each $j = 2, \ldots, N$. To this end, we define the homogeneous adjoint problem $\mathcal{L}_0{}^\star\Psi = 0$ by

$$\mathcal{L}_0^\star\Psi \equiv L_0\Psi - w\frac{\int_0^\infty \rho w^2\Psi\, d\rho}{\int_0^\infty \rho w^2\, d\rho} = 0\,. \tag{4.38}$$

In the class of radially symmetric functions, the nullspace of $\mathcal{L}_0^\star$ is one-dimensional, and is given by (see [35])

$$\Psi^\star \equiv w + \frac{1}{2}\rho w'\,. \tag{4.39}$$

In fact, by a direct calculation, and using $L_0 w = w^2$ together with integration by parts, we readily derive the identities

$$L_0\Psi^\star = w\,, \qquad \int_0^\infty \rho w^2\Psi^\star\, d\rho = \int_0^\infty \rho\,(L_0 w)\left(L_0^{-1}w\right)\, d\rho = \int_0^\infty \rho w^2\, d\rho = b\,, \tag{4.40}$$

which confirms $\mathcal{L}_0^\star\Psi^\star = 0$. From the Fredholm alternative, we conclude that a necessary condition for (4.37a) to have a solution is that $\int_0^\infty \rho\Psi^\star\mathcal{F}_j\, d\rho = 0$. By using (4.37b) for $\mathcal{F}_j$, this solvability condition yields

$$\lambda_1\left(\frac{\int_0^\infty \rho w\Psi^\star\, d\rho}{\int_0^\infty \rho w^2\Psi^\star\, d\rho} + \frac{f}{2(1-f)}\right) = \frac{3}{b(1-f)}\left(\frac{\int_0^\infty \rho w^2 u_{1p}\Psi^\star\, d\rho}{\int_0^\infty \rho w^2\Psi^\star\, d\rho}\right) + \left(-\pi\kappa_{0j} + \frac{\chi_1}{\chi_0} - \frac{3}{2b^2(1-f)}\int_0^\infty \rho w^2 u_{1p}\, d\rho\right)\,. \tag{4.41}$$

Next, we simplify (4.41) by deriving three identities. We first use integration by parts to calculate

$$\int_0^\infty \rho w \Psi^\star \, d\rho = \int_0^\infty \rho w \left(w + \frac{1}{2}\rho w' \right) \, d\rho = \int_0^\infty \rho w^2 \, d\rho + \frac{1}{4}\int_0^\infty \rho^2 \left(w^2\right)' \, d\rho = b - \frac{1}{2}\int_0^\infty \rho w^2 \, d\rho = \frac{b}{2} \,. \tag{4.42a}$$

Next, we use $L_0 v_{1p} = w^2 u_{1p}$ from the perturbation of the core problem (3.1d), together with $L_0 v_{1p} = \rho^{-1}\left(\rho v_{1p}'\right)' - v_{1p} + 2w v_{1p}$, to explicitly calculate that

$$\begin{aligned} &\int_0^\infty \rho w^2 u_{1p} \Psi^\star \, d\rho = \int_0^\infty \rho \left(L_0 v_{1p}\right) \left(L_0^{-1} w\right) \, d\rho = \int_0^\infty \rho w v_{1p} \, d\rho \,, \\ &\int_0^\infty \rho w^2 u_{1p} \, d\rho = \int_0^\infty \rho \left(L_0 v_{1p}\right) \, d\rho = \int_0^\infty \left[\left(\rho v_{1p}'\right)' - \rho v_{1p} + 2\rho w v_{1p} \right] \, d\rho = -\int_0^\infty \rho v_{1p} \, d\rho + 2\int_0^\infty \rho w v_{1p} \, d\rho \,. \end{aligned} \tag{4.42b}$$

Then, we substitute (4.42) into (4.41), and solve for λ_1 to get

$$\lambda_1 = 2\left(1-f\right)\left(-\pi\kappa_{0j} + \frac{\chi_1}{\chi_0} + \frac{3}{2b^2(1-f)}\int_0^\infty \rho v_{1p} \, d\rho \right) \,. \tag{4.43}$$

Finally, we use (3.1e) to calculate χ_1/χ_0 in terms of S_1/S_0, and ultimately in terms of the relative perturbation D_1/D_{0c} in the inhibitor diffusivity from (4.2). By using (3.1e), together with $\chi_0 = S_0 = \sqrt{b(1-f)}/f$ from (4.15), and recalling (4.2), we calculate

$$\frac{\chi_1}{\chi_0} = -\frac{S_1}{S_0} - \frac{1}{b^2(1-f)}\int_0^\infty \rho v_{1p} \, d\rho = \frac{D_1}{2D_{0c}} - \frac{1}{b^2(1-f)}\int_0^\infty \rho v_{1p} \, d\rho \,. \tag{4.44}$$

Upon substituting (4.44) into (4.43), and recalling that $\lambda \sim \nu\lambda_1$, we obtain our main result (4.3a) of Proposition 4.1.

We now show that these zero-eigenvalue crossings for the asynchronous modes correspond to bifurcation values of D where asymmetric solution branches of quasi-equilibria, as characterized by spots of different source strengths, bifurcate from the common source strength solution of the nonlinear algebraic system (2.6). To see this, we perturb the common source strength solution $\mathbf{S} = S_c\mathbf{e}$ of (2.6), by setting $\mathbf{S} = S_c\mathbf{e} + \mathbf{v}$ where $\mathbf{v} \ll 1$. Assuming that the symmetry condition $\mathcal{G}_0\mathbf{e} = \kappa_{01}\mathbf{e}$ of (2.7) holds, we readily derive that $\mathbf{v}$ must satisfy the linearized problem

$$\mathcal{K}\mathbf{v} = \mathbf{0} \,, \qquad \mathcal{K} \equiv (\mathcal{I}-\mathcal{E})\mathcal{G}_0 + \frac{1}{2\pi\nu}\left(\mathcal{I} + \nu\chi'(S_c)(\mathcal{I}-\mathcal{E})\right) \,, \quad \text{where} \quad S_c \equiv \frac{|\Omega|}{2\pi N\sqrt{D}} \,. \tag{4.45}$$

We now show that the critical values of D for which $\mathcal{K}$ has a non-trivial nullspace coincide with the zero-eigenvalue crossing values for D as given in (4.4). Since $\mathcal{G}_0$ is a symmetric matrix and (2.7) holds, it follows upon using $(\mathcal{I}-\mathcal{E})\mathbf{e} = \mathbf{0}$ and $(\mathcal{I}-\mathcal{E})\mathbf{q} = \mathbf{q}$ for any $\mathbf{q}$ with $\mathbf{q}^T\mathbf{e} = 0$, that the eigenspace of $\mathcal{K}$ can be decomposed into the orthogonal subspaces $\mathcal{Q}^\perp$ and $\mathcal{Q}^\parallel$ as defined in (4.29). For $\mathbf{v}^\parallel = \mathbf{e} \in Q^\parallel$, for which $(\mathcal{I}-\mathcal{E})\mathbf{v}^\parallel = \mathbf{0}$, we calculate from (4.45) that $\mathcal{K}\mathbf{v}^\parallel = (2\pi\nu)^{-1}\,\mathbf{v}^\parallel$. Therefore, $\mathbf{v}^\parallel$ can never be an element of the nullspace of $\mathcal{K}$ for any D. Alternatively, if $\mathbf{v} = \mathbf{q}_j \in \mathcal{Q}^\perp$, for which $(\mathcal{I}-\mathcal{E})\mathbf{q}_j = \mathbf{q}_j$, we calculate from (4.45) that

$$\mathcal{K}\mathbf{q}_j = \left(\kappa_{0j} + \frac{1}{2\pi}\chi'(S_c) + \frac{1}{2\pi\nu} \right)\mathbf{q}_j \,, \quad j = 2, \ldots, N \,. \tag{4.46}$$

Therefore, $\mathbf{q}_j$ is in the nullspace of $\mathcal{K}$, whenever D satisfies

$$\kappa_{0j} + \frac{1}{2\pi}\chi'(S_c) + \frac{1}{2\pi\nu} = 0 \,, \tag{4.47}$$

for some j in $j = 2, \ldots, N$. Since $\nu \ll 1$, (4.47) has a solution only when $\chi'(S_c) = \mathcal{O}(\nu^{-1})$, which implies that $S_c \ll 1$, or equivalently $D \gg 1$ from (4.45). By re-writing the expansion for χ in (3.1a) in terms of $S \ll 1$, instead of $\nu \ll 1$, we readily obtain

$$\chi(S) \sim \frac{\hat{\chi}_0}{S} + S\hat{\chi}_1 + \cdots \,, \quad \text{as} \quad S \to 0 \,; \qquad \hat{\chi}_0 = \frac{(1-f)b}{f^2} \,, \qquad \hat{\chi}_1 = -\frac{1}{b^2(1-f)}\int_0^\infty \rho v_{1p} \, d\rho \,. \tag{4.48}$$

Upon differentiating (4.48) at $S = S_c$, where S_c is given in (4.45), we conclude from (4.47) that for $D = D_0/\nu + D_1 + \cdots \gg 1$

$$\frac{1}{\nu} - \frac{4\pi^2 N^2 \hat{\chi}_0}{\nu|\Omega|^2}\left(D_0 + \nu D_1 + \cdots\right) + \hat{\chi}_1 + 2\pi\kappa_{0j} = 0\,. \tag{4.49}$$

We equate the $\mathcal{O}(\nu^{-1})$ and $\mathcal{O}(1)$ terms in (4.49), and use (4.48) for $\hat{\chi}_0$ and $\hat{\chi}_1$. In this way, we get

$$D_0 = D_{0c} \equiv \frac{|\Omega|^2 f^2}{4\pi^2 N^2 b(1-f)}\,, \qquad D_1 = D_{0c}\left(2\pi\kappa_{0j} - \frac{1}{b^2(1-f)}\int_0^\infty \rho v_{1p}\, d\rho\right)\,, \tag{4.50}$$

which agrees with the result in (4.4) for zero-eigenvalue crossings.

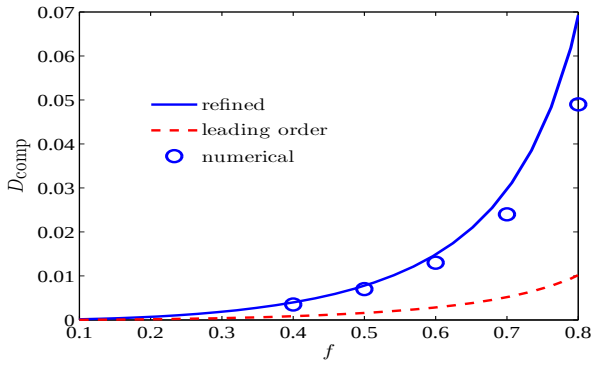

Figure 3: Plot of competition instability threshold versus the Brusselator parameter f when $\varepsilon = 0.01$ and $\tau = 0.002$ for a four-spot ring pattern in the unit disk with ring radius $r_0 = 0.5986$. Top curve is the refined two-term expansion $D_{comp,\varepsilon}$ from (4.5) of Proposition 4.2, while the dotted lower curve is the leading-order threshold D_{0c}/ν from (3.16) of Proposition 3.2. The open circles are the largest values of D for which the four-spot pattern is stable in the PDE simulations of (1.1) using FlexPDE6 [9]. The asymptotic theory predicts that the corresponding mode of instability for the spot amplitudes is the alternating $(1,-1,1,-1)$ mode.

This analysis shows that to leading order in ν, the emergence of such asymmetric solution branches is predicted to occur at the common bifurcation point $D = D_{0c}/\nu$. Our detailed higher-order analysis, which resolves the degeneracy of the leading-order threshold and leads to (4.4), relies critically on the assumption (2.7) that $\mathbf{e}$ is an eigenvector of $\mathcal{G}_0$. In fact, if the spot configuration is such that $\mathbf{e}$ is not an eigenvector of $\mathcal{G}_0$, we conjecture that the inclusion of higher order terms in ν leads to an imperfection sensitivity in the bifurcation structure of solutions to the nonlinear algebraic system (2.6). This imperfection sensitivity structure is intricate to study in full generality and is beyond the scope of this paper. It was first identified in [24] in the context of three localized spots on the sphere (see Fig. 5–6 in [24]).

4.1 Validation of the Competition Threshold

We now compare our two-term asymptotic result $D_{\rm comp,\varepsilon}$, as given in (4.5) of Proposition 4.2, for the competition instability threshold with corresponding results computed from the full PDE system (1.1) using FlexPDE6 [9]. As an illustration of the asymptotic theory, we take $\tau = 0.002$ and $\varepsilon = 0.01$, and consider a four-spot ring pattern in the unit disk where the spots are chosen to be equally-spaced on a ring of radius $r_0 = 0.5986$. This value of the ring radius corresponds to a steady-state of the slow spot dynamics (cf. [26]). A plot of the initial condition for the FlexPDE6 simulation of (1.1) is shown in Fig. 4(a).

For the unit disk, the Neumann Green's matrix $\mathcal{G}_0$ and its eigenvalues are readily calculated (cf. [12]), so as to identify $\kappa_{\rm min}$ in (4.5). Moreover, the core solution w, together with the correction v_{1p} to the core problem, as needed in (4.5), are also easily computed numerically using a BVP solver for a fixed Brusselator parameter f. In this way, in Fig. 3 we compare our two-term threshold $D_{\rm comp,\varepsilon}$ of (4.5) with both the leading-order threshold D_{0c}/ν from (3.16) and with full numerical results for the largest value of D for which the spot pattern is still stable, as computed from FlexPDE6 [9]. From this figure, we observe that the two-term result provides a much more accurate prediction of the competition stability threshold than does the leading order asymptotic theory at our chosen value $\varepsilon = 0.01$.

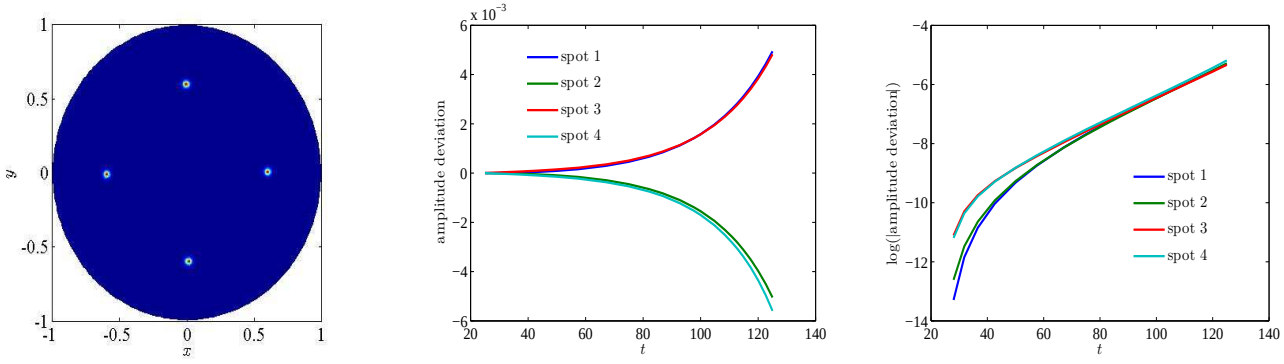

(a) (b) (c)

Figure 4: (a): A surface plot of the initial condition for v with four spots spaced equally on a concentric ring of radius $r_0 = 0.5986$, being the equilibrium ring radius for a four-spot pattern. (b): deviations of the spot amplitudes from quasi-steady state at the initial onset of a competition instability. Spot 1 corresponds to the spot located on the positive x-axis in (a). The numbering increases in the counterclockwise direction. We observe that the amplitudes of Spots 1 and 3 increase, while those of Spots 2 and 4 decrease. Further, the sum of the deviations is close to 0, and the deviations all grow exponentially at approximately the same rate. These observations are all in accordance with the fact that the critical eigenmode is $(1, -1, 1, -1)^T$. (c): the logarithm of the absolute values of the amplitude deviation. The linear behavior indicates exponential growth, while the close proximity of the curves indicate approximately equal growth rates. The parameters are: $f = 0.6$, $D = 0.014$, $\varepsilon = 0.01$, and $\tau = 0.002$.

By identifying the specific eigenvector of $\mathcal{G}_0$ that corresponds to $\kappa_{\min}$, our asymptotic theory predicts that the spatial mode of linear instability for the spot amplitudes is the alternating $(1, -1, 1, -1)$ mode. For $f = 0.6$, this prediction is confirmed from the FlexPDE6 results for the full PDE system (1.1) shown in Fig. 4(b) and Fig. 4(c), where for a chosen D slightly above the stability threshold we observe that the spot amplitudes for one pair of antipodal spots grows, while the other pair decays, as time increases. For this example, our refined asymptotic theory provides a close determination of the competition stability threshold and accurately predicts the spatial mode of instability for the spot amplitudes.

5 Refined Stability Threshold for Periodic Spot Patterns

In this section we study the linear stability on an $\mathcal{O}(1)$ time-scale of steady-state periodic spot patterns for the Brusselator (1.1) when the spots are centered in the limit $\epsilon \to 0$ at the lattice points of a general oblique Bravais lattice Λ with fixed area $|\Omega|$ of the fundamental Wigner-Seitz cell Ω. These $\mathcal{O}(1)$ time-scale instabilities are instabilities in the spot amplitudes. For this periodic problem, and to leading-order in ν, the linearization of the periodic spot equilibria, corresponding to spot amplitude perturbations, has a zero eigenvalue when $D = D_{0c}/\nu$, where D_{0c} is given by

$$D_{0c} = \frac{|\Omega|^2 f^2}{4\pi^2 b(1-f)}, \qquad b \equiv \int_0^\infty \rho w^2 \, d\rho \,. \tag{5.1}$$

For the analogous finite-domain problem considered in §4, and under the symmetry condition (2.7) on the spot configuration $\{\mathbf{x}_1, \ldots, \mathbf{x}_N\}$, such a zero-eigenvalue crossing was shown to correspond to a competition instability of the spot amplitudes. Our goal here is to extend the analysis in §4 for the unfolding of this zero eigenvalue for the finite-domain problem to the case of a periodic pattern of spots in $\mathbb{R}^2$, in order to obtain a result analogous to that in Proposition 4.1.

Before giving our main linear stability result for the periodic case, we recall a few basic facts about Bravais lattices and their duals. The Bravais lattice Λ is defined in terms of two independent vectors, or generators, $\boldsymbol{l}_1$ and $\boldsymbol{l}_2$ in $\mathbb{R}^2$ by

$$\Lambda = \left\{ m\boldsymbol{l}_1 + n\boldsymbol{l}_2 \;\middle|\; m, n \in \mathbb{Z} \right\}, \tag{5.2}$$

where $\mathbb{Z}$ denotes the set of integers. For convenience, $\boldsymbol{l}_1$ is taken to be aligned with the positive x_1-axis, and θ is the angle between $\boldsymbol{l}_1$ and $\boldsymbol{l}_2$. The *Wigner-Seitz* (WS), or Voronoi, cell centered at a given lattice point of Λ consists of all points in the plane that are closer to this point than to any other lattice point. The union of the WS cells tile all of $\mathbb{R}^2$,

i.e. $\mathbb{R}^2 = \bigcup_{z\in\Lambda}(z+\Omega)$, where Ω is the fundamental WS cell centered at the origin $\mathbf{x}=\mathbf{0}$. A schematic plot of the union of the WS cells for a specific Bravais lattice is shown in Fig. 5.

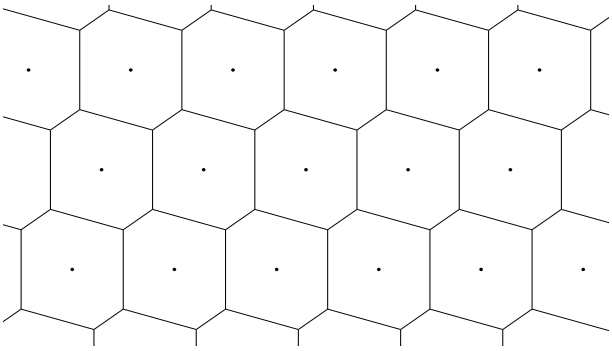

Figure 5: WS cells for an oblique Bravais lattice with generators $\boldsymbol{l}_1 = (1,0)$, $\boldsymbol{l}_2 = (\cot\theta, 1)$, and $\theta = 74^\circ$, so that $|\Omega| = 1$. These cells tile $\mathbb{R}^2$. The boundary of the WS cells generically (except for the square) consist of three pairs of parallel lines of equal length.

Following [4], the reciprocal or dual lattice $\Lambda^\star$ is defined in terms of two independent vectors $\boldsymbol{d}_1$ and $\boldsymbol{d}_2$, which are obtained from the lattice Λ by requiring that

$$\boldsymbol{d}_i \cdot \boldsymbol{l}_j = \delta_{ij}\,, \tag{5.3}$$

where δ_{ij} is the Kronecker symbol. The reciprocal lattice $\Lambda^\star$ is then defined by

$$\Lambda^\star = \left\{ m\boldsymbol{d}_1 + n\boldsymbol{d}_2 \;\middle|\; m,\, n \in \mathbb{Z} \right\}. \tag{5.4}$$

The first Brillouin zone, labeled by Ω_B, is defined as the WS cell centered at the origin in the reciprocal space.

For the periodic spot problem, we will derive the following main result characterizing the continuous band of spectrum of the linearization satisfying $|\lambda| = \mathcal{O}(\nu)$ when $D = D_{0c}/\nu + D_1 + o(1)$:

Proposition 5.1 *In the limit $\epsilon \to 0$, consider a steady-state periodic pattern of spots for the Brusselator (1.1) in $\mathbb{R}^2$, where the spots are centered at the lattice points of a Bravais lattice Λ with a fixed area $|\Omega|$ of the fundamental WS cell. Then, for the de-tuning $D = D_{0c}/\nu + D_1 + o(1)$, where D_{0c} is given in (5.1), the portion of the continuous spectrum of the linearization, corresponding to spot amplitude perturbations, that satisfies $|\lambda| \le \mathcal{O}(\nu) \ll 1$, is given by*

$$\lambda = 2\nu(1-f)\nu\left[-\pi R_{b0}(\boldsymbol{k}) + \frac{D_1}{2D_{0c}} + \frac{1}{2b^2(1-f)}\int_0^\infty \rho v_{1p}\, d\rho\right] + o(\nu)\,, \tag{5.5}$$

where v_{1p} is defined in (3.1d) and $\nu = -1/\log\varepsilon$. Here $R_{b0}(\boldsymbol{k})$ is the regular part of the Bloch Green's function G_{b0} for the Laplacian, with $\boldsymbol{k}/(2\pi) \in \Omega_B\backslash\{\mathbf{0}\}$, satisfying

$$\Delta G_{b0} = -\delta(\mathbf{x})\,; \qquad G_{b0}(\mathbf{x}+\boldsymbol{l}) = e^{-i\boldsymbol{k}\cdot\boldsymbol{l}}\, G_{b0}(\mathbf{x})\,, \qquad \boldsymbol{l} \in \Lambda\,, \tag{5.6a}$$

where $R_{b0}(\boldsymbol{k})$ is defined by

$$R_{b0}(\boldsymbol{k}) \equiv \lim_{\mathbf{x}\to\mathbf{0}}\left(G_{b0}(\mathbf{x}) + \frac{1}{2\pi}\log|\mathbf{x}| \right). \tag{5.6b}$$

In order to more explicitly characterize the continuous band of spectra in (5.5), we require two key properties of $R_{b0}(\boldsymbol{k})$. The following result, as rigorously established in Lemmas 2.1 and 2.2 of [10], is central to the discussion below.

Lemma 5.2 *[From [10]]: The regular part $R_{b0}(\boldsymbol{k})$ of $G_{b0}(\mathbf{x})$, defined in (5.6b), is real-valued for $|\boldsymbol{k}| \neq 0$. In addition, for $|\boldsymbol{k}| \to \mathbf{0}$, $R_{b0}(\boldsymbol{k})$ has the singular asymptotic behavior*

$$R_{b0}(\boldsymbol{k}) \sim \frac{1}{\boldsymbol{k}^T\mathcal{Q}\boldsymbol{k}} = \mathcal{O}(|\mathcal{Q}^{1/2}\boldsymbol{k}|^{-2}) \gg 1\,, \quad \text{as} \quad |\boldsymbol{k}| \to 0\,, \tag{5.7}$$

where $\mathcal{Q}$ is a certain positive-definite matrix defined in terms of the lattice generators.

Since $R_{b0}(\boldsymbol{k})$ is real-valued, (5.5) shows that the band of spectrum satisfying $|\lambda| = \mathcal{O}(\nu) \ll 1$ when $D = D_{0c}/\nu + D_1 + o(1)$ is real-valued. Therefore, to determine the stability threshold for a given lattice Λ, we need only locate the right-most edge $\lambda_{\rm edge}$ of the band as $\boldsymbol{k}/(2\pi)$ is varied in the first Brillouin zone Ω_B, and ensure that this leading edge satisfies $\lambda_{\rm edge} < 0$. Although (5.5) is not uniformly valid as $\boldsymbol{k} \to 0$, owing to the fact that $R_{b0} = \mathcal{O}(|\mathcal{Q}^{1/2}\boldsymbol{k}|^{-2}) \to +\infty$ as $|\boldsymbol{k}| \to 0$ (see (5.7)), we observe that $\lambda < 0$ for $\mathcal{O}(\nu^{1/2}) \ll |\boldsymbol{k}| \ll 1$. Therefore, long-wavelength perturbations do not determine the stability threshold. A schematic plot of the spectrum near the origin is shown in Fig. 6.

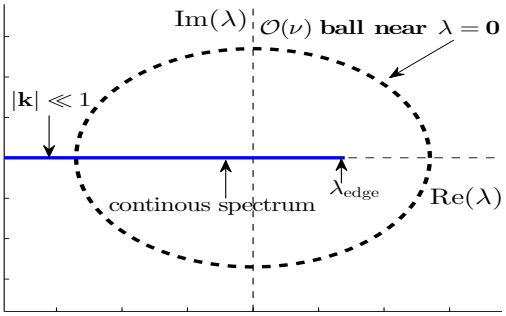

Figure 6: Continuous band of real-valued spectra within the small ball $|\lambda| = \mathcal{O}(\nu)$. For a given Bravais lattice Λ, the de-tuning parameter D_1 is chosen small enough to ensure that the edge λ_{edge} of this band satisfies $\lambda_{edge} < 0$. The optimal lattice then maximizes this critical value $D_1^\star$ for D_1.

By detecting the right-most edge of the band of spectra, we conclude from (5.5) that a periodic pattern of spots on a fixed lattice Λ is linearly stable to spot amplitude perturbations when

$$D_1 < D_1^\star \equiv D_{0c}\left[2\pi R_{b0}^\star - \frac{1}{b^2(1-f)}\int_0^\infty \rho v_{1p}\, d\rho\right], \qquad R_{b0}^\star \equiv \min_{\boldsymbol{k}/(2\pi)\in\Omega_B} R_{b0}(\boldsymbol{k})\,. \tag{5.8}$$

Then, for a fixed area $|\Omega|$ of the WS cell, we define the *optimal* lattice Λ as the one that maximizes $D_1^\star$ over all oblique Bravais lattices. This optimal lattice is the one which provides the largest range of D for which the periodic spot pattern is linearly stable to spot amplitude perturbations. The result is as follows:

Proposition 5.3 *The optimal arrangement of a periodic pattern of spots for the Brusselator (1.1) is the one for which $R_{b0}^\star$ is maximized over the class of Bravais lattices (5.2) with fixed area $|\Omega|$ of the fundamental WS cell. A two-term asymptotic expansion for this optimal stability threshold for D, associated with spot amplitude perturbations, is*

$$D_{optim} \sim \frac{D_{0c}}{\nu}\left[1 + \nu\left(2\pi \max_{\Lambda} R_{b0}^\star - \frac{1}{b^2(1-f)}\int_0^\infty \rho v_{1p}\, d\rho\right)\right], \qquad R_{b0}^\star \equiv \min_{\boldsymbol{k}/(2\pi)\in\Omega_B} R_{b0}(\boldsymbol{k})\,, \tag{5.9}$$

where $\nu = -1/\log\varepsilon$ and D_{0c} is given in (5.1), Here $R_{b0}(\boldsymbol{k})$ satisfies (5.6b), v_{1p} is defined in (3.1d), and $b \equiv \int_0^\infty w^2\rho\, d\rho$ where $w(\rho) > 0$ is the ground-state solution of (3.1c).

In order to numerically identify the optimal lattice through the max-min characterization in Proposition 5.3, an explicit and rapidly converging infinite series representation for $R_{b0}(\boldsymbol{k})$ is required. This was done in §6 of [10] using an Ewald-type summation procedure resulting from the Poisson summation formula, as motivated by [4]. From §6 of [10], we have

$$R_{b0}(\boldsymbol{k}) = \sum_{\boldsymbol{d}\in\Lambda^*} \exp\left(-\frac{|2\pi\boldsymbol{d}-\boldsymbol{k}|^2}{4\eta^2}\right)\frac{1}{|2\pi\boldsymbol{d}-\boldsymbol{k}|^2} + \sum_{\substack{\boldsymbol{l}\in\Lambda\\ \boldsymbol{l}\neq\boldsymbol{0}}} e^{i\boldsymbol{k}\cdot\boldsymbol{l}}\, F_{\rm sing}(\boldsymbol{l}) - \frac{\gamma_e}{4\pi} - \frac{\log\eta}{2\pi}\,, \tag{5.10}$$

where $F_{\rm sing}(\boldsymbol{l}) = E_1(|\boldsymbol{l}|^2\eta^2)/(4\pi)$, $E_1(z) = \int_z^\infty t^{-1}e^{-t}\,dt$ is the exponential integral (cf. §5.1.1 of [1]), and γ_e is Euler's constant. Here $\eta > 0$ is an Ewald cut-off parameter, used to ensure rapid convergence of the two infinite sums in (5.10) over the lattice and its dual. By using this explicit representation of $R_{b0}(\boldsymbol{k})$ in [10] (see Fig. 5 and Fig. 7 in [10]), a numerical sweep in $\boldsymbol{k}/(2\pi)$ over the first Brillouin zone Ω_B, together with a sweep over the class of Bravais lattices with $|\Omega| = 1$, has numerically identified that $R_{b0}^\star$ is maximized for a regular hexagonal lattice.

5.1 Derivation of the Spectral Estimate in Proposition 5.1

We use the method of matched asymptotic expansions to construct a steady-state spot solution for the Brusselator (1.1) centered at the origin of the fundamental WS cell Ω. This solution in Ω can then be periodically extended to the lattice.

In the $\mathcal{O}(\epsilon)$ core of the spot centered at $\mathbf{x}=\mathbf{0}$ we let $u = D^{-1/2}U(\rho)$ and $v = D^{1/2}V(\rho)$, with $\mathbf{y} = \epsilon^{-1}\mathbf{x}$ and $\rho \equiv |\mathbf{y}|$, to obtain the radially symmetric core problem

$$\begin{aligned} &\Delta_\rho V - V + fUV^2 = 0\,, \qquad \Delta_\rho U + V - UV^2 = 0\,, \qquad \rho \equiv |\mathbf{y}| > 0\,, \\ &U'(0) = V'(0) = 0\,; \qquad V \to 0\,, \qquad U \sim S\log\rho + \chi(S) \quad \text{as} \quad \rho \to \infty\,. \end{aligned} \tag{5.11}$$

In the outer region, we have $v \sim \varepsilon^2$. Moreover, in analogy with (2.2a), the outer problem for u, which matches the far-field behavior of the core solution U in (5.11), is

$$D\Delta u = -1 + 2\pi\sqrt{D}S\delta(\mathbf{x})\,, \quad \mathbf{x}\in\Omega\,; \qquad \mathcal{P}_0 u = 0\,, \quad \mathbf{x}\in\partial\Omega\,, \tag{5.12a}$$

$$u \sim D^{-1/2}\left(S\log|\mathbf{x}| + S/\nu + \chi(S)\right) \quad \text{as} \quad \mathbf{x}\to\mathbf{0}\,, \tag{5.12b}$$

where $\nu \equiv -1/\log\epsilon \ll 1$. Here the boundary operator $\mathcal{P}_0 u = 0$ denotes periodic boundary conditions on $\partial\Omega$. By integrating over Ω, the divergence theorem yields that

$$S = \frac{|\Omega|}{2\pi\sqrt{D}}\,. \tag{5.13}$$

To solve (5.12), we introduce the periodic Green's function $G_p(\mathbf{x})$ and its regular part R_p by

$$\begin{aligned} &\Delta G_p = \frac{1}{|\Omega|} - \delta(\mathbf{x})\,, \quad \mathbf{x}\in\Omega\,; \qquad \mathcal{P}_0 G_p = 0\,, \quad \mathbf{x}\in\partial\Omega\,; \\ &\int_\Omega G_p\, d\mathbf{x} = 0\,, \qquad G_p = -\frac{1}{2\pi}\log|\mathbf{x}| + R_p + o(1) \quad \text{as} \quad \mathbf{x}\to\mathbf{0}\,. \end{aligned} \tag{5.14}$$

For S as given in (5.13), the solution to (5.12) is

$$u = -\frac{2\pi S}{\sqrt{D}}G_p(\mathbf{x}) + \bar{u}\,, \qquad \text{where} \quad \bar{u} = \frac{1}{\sqrt{D}}\left[\frac{S}{\nu} + \chi(S) + 2\pi S R_p\right]\,. \tag{5.15}$$

This completes the construction of the steady-state spot solution in Ω, which is then extended periodically to the lattice.

Next, we formulate the linear stability problem for a periodic pattern of spots in $\mathbb{R}^2$ by using the Floquet-Bloch theorem. As shown in [10], the quasi-periodicity condition for the linearization around the steady-state spot pattern from the Floquet-Bloch theorem can be formulated in terms of a boundary operator $\mathcal{P}_k$ on the boundary $\partial\Omega$ of the WS cell involving the Bloch wavevector $\boldsymbol{k}$ (see equation (2.35) of [10])

We let v_e and u_e denote the steady-state spot solution in Ω, and in (1.1) we introduce the perturbation

$$v = v_e + e^{\lambda t}\phi\,, \qquad u = u_e + e^{\lambda t}\eta\,, \tag{5.16}$$

where $|\phi| \ll 1$ and $\eta \ll 1$, This yields the following eigenvalue problem in the fundamental WS cell Ω

$$\epsilon^2\Delta\phi - \phi + 2fu_e v_e\phi + fv_e^2\eta = \lambda\phi\,, \quad \mathbf{x}\in\Omega\,, \qquad \mathcal{P}_k\phi = 0\,, \quad \mathbf{x}\in\partial\Omega\,, \tag{5.17a}$$

$$D\Delta\eta + \frac{1}{\epsilon^2}\left(\phi - 2u_e v_e\phi - v_e^2\eta\right) = \tau\lambda\eta\,, \quad \mathbf{x}\in\Omega\,, \qquad \mathcal{P}_k\eta = 0\,, \quad \mathbf{x}\in\partial\Omega\,. \tag{5.17b}$$

Near the core of the spot, we have $v_e \sim D^{1/2}V$ and $u_e \sim D^{-1/2}U$, with $\mathbf{y} = \epsilon^{-1}\mathbf{x}$ and $\rho = |\mathbf{y}|$, where $U(\rho)$ and $V(\rho)$ satisfy the core problem (5.11). In the inner region, we introduce the locally radially symmetric eigenfunction

$$\phi(\mathbf{x}) \sim D\Phi(\rho)\,, \qquad \eta(\mathbf{x}) \sim N(\rho)\,. \tag{5.18}$$

Then, from (5.17), and assuming that the consistency condition (2.13) holds, we obtain on $\rho \geq 0$ that

$$\Delta_\rho \Phi - \Phi + 2fUV\Phi + fV^2 N = \lambda \Phi\,, \qquad \Phi \to 0 \quad \text{as} \quad \rho \to \infty\,, \tag{5.19a}$$

$$\Delta_\rho N + (1 - 2UV)\,\Phi - V^2 N = 0\,, \qquad N \sim C\log\rho + B\,, \quad \text{as} \quad \rho \to \infty\,, \tag{5.19b}$$

where $\Delta_\rho \equiv \partial_{\rho\rho} + \rho^{-1}\partial_\rho$. Since (5.19) is linear and homogeneous, we can write

$$B = C\hat{B}\,, \tag{5.20}$$

where $\hat{B} = \hat{B}(\lambda, S)$ must be computed numerically from (5.19)

In analogy with (2.15), the outer problem for η whose singularity behavior matches the far-field behavior of N is

$$\Delta\eta - \frac{\tau\lambda}{D}\eta = 2\pi C\delta(\mathbf{x})\,, \quad \mathbf{x} \in \Omega\,, \qquad \mathcal{P}_k\eta = 0\,, \quad \mathbf{x} \in \partial\Omega\,, \tag{5.21a}$$

$$\eta \sim C\log|\mathbf{x}| + \frac{C}{\nu} + B \quad \text{as} \quad \mathbf{x} \to \mathbf{0}\,. \tag{5.21b}$$

To solve (5.21), we introduce the eigenvalue-dependent Bloch Green's function $G_{b,\lambda}(\mathbf{x})$ in Ω satisfying

$$\begin{aligned} &\Delta G_{b,\lambda} - \frac{\tau\lambda}{D}G_{b,\lambda} = -\delta(\mathbf{x})\,, \quad \mathbf{x} \in \Omega\,; \qquad \mathcal{P}_k G_{b,\lambda} = 0\,, \quad \mathbf{x} \in \partial\Omega\,; \\ &G_{b,\lambda} \sim -\frac{1}{2\pi}\log|\mathbf{x}| + R_{b,\lambda} + o(1) \quad \text{as} \quad \mathbf{x} \to \mathbf{0}\,. \end{aligned} \tag{5.22}$$

From the Floquet boundary operator $\mathcal{P}_k$, both $G_{b,\lambda}(\mathbf{x})$ and its regular part $R_{b,\lambda}$ depend on the Bloch wavevector $\boldsymbol{k}$. In terms of this Green's function, the solution to (5.21) is $\eta = -2\pi C G_{b,\lambda}(\mathbf{x})$. By enforcing the singularity condition (5.21b) we conclude that

$$(1 + 2\pi\nu R_{b,\lambda})\,C + \nu B = 0\,. \tag{5.23}$$

Since $B = \hat{B}C$ from (5.20), (5.23) yields the transcendental equation $1 + 2\pi\nu R_{b,\lambda} + \nu\hat{B} = 0$ for the spectrum of the linearization parameterized by the Bloch wavevector $\boldsymbol{k}$.

This asymptotic construction of the steady-state solution and the formulation of the linear stability problem in (5.23) is accurate to all powers in ν. From this formulation, we now derive the explicit asymptotic result in (5.5) for the spectrum of the linearization within the small ball $|\lambda| = \mathcal{O}(\nu) \ll 1$ for the range $D = D_{0c}/\nu + D_1 + o(1)$, where D_{0c} is the leading-order stability threshold given in (5.1). This analysis will yield the two-term-in-ν asymptotic result for the critical stability threshold for D as given in (5.8).

To do so, we need to analyze (5.19), (5.23), and the core problem (5.11), for the regime $D = D_0/\nu$. For this range, we have from (5.13) that

$$S = S_0\nu^{1/2} + S_1\nu + \cdots\,, \qquad \text{where} \qquad S_0 = \frac{|\Omega|}{2\pi\sqrt{D_{0c}}}\,, \qquad S_1 = -\frac{D_1}{2D_{0c}}S_0\,. \tag{5.24}$$

Moreover, we obtain from Lemma 3.1, that a two-term expansion for the solution to the core problem (5.11) is

$$V \sim \nu^{1/2}\left(\frac{w}{f\chi_0} - \nu\left(\frac{\chi_1 w}{f\chi_0^2} + \frac{v_{1p}}{f^3\chi_0^3}\right) + \cdots\right)\,, \tag{5.25a}$$

$$U \sim \nu^{-1/2}\left(\chi_0 + \nu\left(\chi_1 + \frac{u_{1p}}{f^2\chi_0}\right) + \cdots\right)\,, \qquad \chi \sim \nu^{-1/2}\left(\chi_0 + \nu\chi_1 + \cdots\right)\,. \tag{5.25b}$$

Here $b \equiv \int_0^\infty \rho w^2\,d\rho$, $w(\rho)$ is the ground-state of (3.1c), v_{1p} and u_{1p} satisfy (3.1d), while χ_0 and χ_1 are defined in (3.1e).

For $\lambda = \nu\lambda_1 + o(\nu)$ and $D = D_{0c}/\nu + D_1 + o(1)$, we readily obtain that (5.23) reduces to

$$\left(1 + 2\pi\nu R_{b,0} + \mathcal{O}(\nu^3)\right)C + \nu B = 0\,. \tag{5.26}$$

Here $R_{b,0}$ is the regular part of the Bloch Green's function defined in (5.6). We then expand Φ, N, C, and B, in (5.19) and (5.26) as

$$\Phi = \nu\left(\Phi_0 + \nu\Phi_1 + \cdots\right)\,, \quad N = N_0 + \nu N_1 + \nu^2 N_2 + \cdots\,, \quad B = B_0 + \nu B_1 + \nu^2 B_2 + \cdots\,, \quad C = \nu\left(C_0 + \nu C_1 + \cdots\right)\,. \tag{5.27}$$

By substituting these expansions for C and B into (5.26), and then collecting powers of ν, we conclude that

$$C_0 = -B_0\,, \qquad C_1 = 2\pi R_{b,0} B_0 - B_1\,. \tag{5.28}$$

Next, we substitute (5.27) and (5.25) into (5.19) and collect powers of ν to obtain problems at each order. Since this part of the calculation is similar to that in §4, we only sketch the analysis here. At leading order, we get that

$$L_0\Phi_0 + \frac{w^2}{f\chi_0^2} N_0 = 0\,, \quad \mathbf{\Phi}_0 \to 0 \quad \text{as} \quad \rho \to \infty\,; \qquad \Delta_\rho N_0 = 0\,, \quad N_0 \sim B_0 \quad \text{as} \quad \rho \to \infty\,. \tag{5.29}$$

Therefore, as similar to (4.8), we conclude that

$$\Phi_0 = -\frac{w}{f\chi_0^2} B_0\,, \qquad B_0 = N_0\,. \tag{5.30}$$

At next order, we obtain that N_1 satisfies

$$\Delta_\rho N_1 = -\left(1 - \frac{2w}{f}\right)\Phi_0 + \frac{w^2}{f^2\chi_0^2} N_0\,, \quad \rho \geq 0\,; \qquad N_1 \sim C_0 \log\rho + B_1 \quad \text{as} \quad \rho \to \infty\,. \tag{5.31a}$$

By applying the divergence theorem, we conclude that

$$C_0 = \frac{b}{f^2\chi_0^2} N_0 + \int_0^\infty \rho\left(\frac{2w}{f} - 1\right)\mathbf{\Phi}_0\, d\rho\,. \tag{5.31b}$$

We then use $C_0 = -B_0$, $N_0 = B_0$, and (5.30) for Φ_0 to obtain from (5.31b) that

$$-B_0 = \frac{B_0}{f^2\chi_0^2}\left(b - \int_0^\infty \rho w(2w - f)\, d\rho\right) = -\frac{B_0 b}{f^2\chi_0^2}\,(1-f)\,,$$

which yields $f^2\chi_0^2 = b(1-f)$. By recalling the relationship between χ_0 and S_0 from (3.1e), and then using (5.24) relating S_0 to D_{0c}, we conclude that

$$\chi_0 = S_0 = \frac{\sqrt{b(1-f)}}{f}\,, \qquad D_{0c} = \frac{|\Omega|^2 f^2}{4\pi^2 b(1-f)}\,. \tag{5.32}$$

This yields the leading-order stability threshold in (5.1). We then substitute (5.30) for Φ_0 and $C_0 = -B_0$ into the problem (5.31a) for N_1 to identify, as was done in (4.17), that

$$N_1 = -\frac{B_0 f}{b(1-f)} u_{1p} + B_1\,, \tag{5.33}$$

where u_{1p} is the correction to the core problem given in (3.1d).

Upon using (5.30) for Φ_0, (5.33) for N_1, and $B_0 = N_0$ in the problem for the second-order correction N_2, we obtain, as similar to (4.21), that N_2 satisfies

$$\begin{aligned} &\Delta N_2 = -\left(1 - \frac{2w}{f}\right)\Phi_1 - \frac{3w^2 u_{1p}}{b^2(1-f)^2} B_0 - \frac{2w^2 f\chi_1}{[b(1-f)]^{3/2}} B_0 + \frac{w^2}{b(1-f)} B_1\,, \quad \rho \geq 0\,, \\ &N_2 \sim C_1 \log\rho + B_2\,, \quad \text{as} \quad \rho \to \infty\,. \end{aligned} \tag{5.34}$$

Upon applying the divergence theorem, we calculate C_1 in (5.34) as

$$C_1 = \int_0^\infty \rho\left(\frac{2w}{f} - 1\right)\Phi_1\, d\rho + \frac{B_1}{(1-f)} - \frac{3B_0}{b^2(1-f)^2}\int_0^\infty \rho w^2 u_{1p}\, d\rho - \frac{2f\chi_1 b}{[b(1-f)]^{3/2}} B_0\,. \tag{5.35}$$

Next, we derive the problem for Φ_1. We substitute (5.27) and (5.25) into the first equation of (5.19), and retain terms of order ν. Then, by using (5.30) for Φ_0 and N_0, together with (5.33) for N_1 and $\chi_0^2 f^2 = b(1-f)$, the problem for Φ_1 reduces to

$$L_0\Phi_1 - \frac{3w^2 f u_{1p}}{b^2(1-f)^2} B_0 + \frac{w^2 f}{b(1-f)} B_1 - \frac{2w^2 f^2\chi_1}{[b(1-f)]^{3/2}} B_0 = -\frac{\lambda_1 f w}{b(1-f)} B_0\,, \qquad \rho \geq 0\,, \tag{5.36}$$

where $\Phi_1 \to \mathbf{0}$ as $\rho \to \infty$, and $L_0\Phi_1 \equiv \Delta_\rho \Phi_1 - \Phi_1 + 2w\Phi_1$. We then integrate (5.36) over $0 < \rho < \infty$ to isolate $\int_0^\infty \rho\Phi_1\, d\rho$ as

$$-\int_0^\infty \rho\Phi_1\, d\rho = -\int_0^\infty 2\rho w\Phi_1\, d\rho + \frac{3fB_0}{b^2(1-f)^2}\int_0^\infty \rho w^2 u_{1p}\, d\rho - \frac{f}{(1-f)}B_1 + \frac{2bf^2\chi_1}{[b(1-f)]^{3/2}}B_0 - \frac{\lambda_1 f}{1-f}B_0\,. \tag{5.37}$$

Upon substituting (5.37) into (5.35), we eliminate $\int_0^\infty \rho\mathbf{\Phi}_1\, d\rho$ and obtain

$$C_1 = \frac{(1-f)}{f}\int_0^\infty 2\rho w\Phi_1\, d\rho + B_1 - \frac{3B_0}{b^2(1-f)}\int_0^\infty \rho w^2 u_{1p}\, d\rho - \frac{2\chi_1 f}{[b(1-f)]^{1/2}}B_0 - \frac{\lambda_1 f}{1-f}B_0\,. \tag{5.38}$$

Since $C_1 = 2\pi R_{b,0}B_0 - B_1$ from (5.28), we can solve (5.38) for B_1 in terms of B_0 to get

$$B_1 = \pi R_{b,0}B_0 - \frac{(1-f)}{f}\int_0^\infty \rho w\Phi_1\, d\rho + \frac{3B_0}{2b^2(1-f)}\int_0^\infty \rho w^2 u_{1p}\, d\rho + \left(\frac{\chi_1 f}{[b(1-f)]^{1/2}} + \frac{\lambda_1 f}{2(1-f)}\right)B_0\,. \tag{5.39}$$

Finally, by using (5.39) to eliminate B_1 in (5.36) we obtain the following perturbed NLEP

$$L_0\Phi_1 - w^2\frac{\int_0^\infty \rho w\Phi_1\, d\rho}{\int_0^\infty \rho w^2\, d\rho} = B_0\mathcal{F}\,, \quad \rho \geq 0\,, \quad \Phi_1 \to 0 \quad \text{as} \quad \rho \to \infty\,, \tag{5.40a}$$

$$\mathcal{F} \equiv -\frac{\lambda_1 f}{b(1-f)}\left(w + \frac{fw^2}{2(1-f)}\right) + \frac{3fw^2u_{1p}}{b^2(1-f)^2} + \frac{w^2 f}{b(1-f)}\left(-\pi R_{b,0} + \frac{\chi_1}{\chi_0} - \frac{3}{2b^2(1-f)}\int_0^\infty \rho w^2 u_{1p}\, d\rho\right)\,. \tag{5.40b}$$

The remainder of the derivation parallels that in (4.38)–(4.44). A necessary condition for (5.40) to have a solution is that $\int_0^\infty \mathcal{F}\Psi^\star\, d\rho = 0$, where $\Psi^\star$ is the homogeneous adjoint solution given in (4.39). By invoking this solvability condition, and then simplifying the resulting expression by using the identities in (4.40) and (4.42), we obtain that

$$\lambda_1 = 2(1-f)\left(-\pi R_{b,0} + \frac{\chi_1}{\chi_0} + \frac{3}{2b^2(1-f)}\int_0^\infty \rho v_{1p}\, d\rho\right)\,. \tag{5.41}$$

The last step in the calculation is to use (4.44) to relate χ_1/χ_0 to the de-tuning parameter ratio $D_1/(2D_{0c})$. This yields

$$\lambda_1 = 2(1-f)\left(-\pi R_{b,0} + \frac{D_1}{2D_{0c}} + \frac{1}{2b^2(1-f)}\int_0^\infty \rho v_{1p}\, d\rho\right)\,, \tag{5.42}$$

Recalling that $\lambda \sim \nu\lambda_1$, (5.42) yields our main result (5.5) of Proposition 5.1.

6 Discussion

For the Brusselator model (1.1) in the parameter regime $D = \mathcal{O}(\nu^{-1})$, where $\nu = -1/\log\varepsilon$, we have extended the conventional leading-order NLEP linear stability theory for spot amplitude instabilities, as initially developed for other RD systems in [32] and [34] (see also [36]), to one-higher order in the logarithmic gauge ν. For a multi-spot pattern on a finite domain under the symmetry condition (2.7), or for a periodic pattern of spots centered at the lattice points of a Bravais lattice in $\mathbb{R}^2$, our extended NLEP theory has provided explicit and improved analytical predictions for the critical value of the inhibitor diffusivity D at which a competition instability, due to a zero-eigenvalue crossing, will occur. However, most importantly, our higher-order analysis also provided a detailed characterization of the spectrum of the linearization of the spot pattern within the small ball $|\lambda| = \mathcal{O}(\nu) \ll 1$ of the spectral plane whenever D is near this instability threshold. For an N-spot pattern on a bounded domain, we have also shown that the conventional leading-order NLEP theory is insufficient for analyzing spot amplitude oscillations, as characterized by a Hopf bifurcation threshold value of τ in (1.1), when D is either near to, or below, the competition instability threshold. For D below the competition threshold, we derived a new NLEP and showed from it that the spot amplitudes will undergo a Hopf bifurcation when $\tau = \tau_H \sim \varepsilon^{-\tau_c}/\nu \gg 1$ for some anomalous threshold $\tau_c > 0$. An explicit formula for τ_c was provided.

We now briefly discuss a few open problems regarding the linear stability analysis for spot patterns on a finite domain. For a specified bounded domain Ω, one key open problem is to numerically identify steady-state configurations of localized

spots, other than simple configurations such as ring-type patterns associated with the disk, for which the symmetry condition (2.7) on the Neumann Green' matrix holds. For an arbitrary domain shape, this study would require a fast solver to compute the Neumann Green's function and its regular part, similar to that developed in [15] for the reduced-wave operator. This numerical methodology would then allow us to rapidly compute the Neumann Green's matrix and its eigenvectors over a large sunspace of possible spot configurations $\{\mathbf{x}_1,\dots,\mathbf{x}_N\}$. Recall that our two-term asymptotic expansion in $\nu=-1/\log\varepsilon$ for the competition stability threshold is valid in an arbitrary bounded 2-D domain whenever (2.7) holds. A second key open problem, given that the zero-eigenvalue crossing for a linear competition instability has now been unfolded, is to use multiple time-scale asymptotics to derive amplitude equations characterizing the weakly nonlinear development of a competition instability. We conjecture that the linear competition instability corresponds to a subcritical bifurcation, since from the full PDE numerical simulations shown in Fig. 4, as well as from the additional numerical results in [26], it is found to trigger a nonlinear process through which spots are annihilated in finite time. Thirdly, it would be interesting to give a detailed analysis of an imperfection-sensitive bifurcation structure of solutions to the nonlinear algebraic system (2.6) that is conjectured to occur near the competition threshold $D=D_{0c}/\nu+D_1$, whenever the symmetry condition (2.7) is violated. Finally, it would be worthwhile to extend the two-term asymptotic theory given in §4 to calculate similar refined predictions of the competition instability threshold for other RD systems with localized spot solutions on a finite domain, such as the Gray-Scott, Schnakenberg, and Gierer-Meinhardt systems.

We conclude by briefly mentioning a few open linear stability problems for spot patterns in the periodic case. For a spot pattern on a Bravais lattice with a fixed area of the fundamental WS cell, a key open issue is to establish analytically, rather than numerically, that the minimum of the regular part $R_{b0}(\boldsymbol{k})$ of the Bloch Green's function over the first Brillouin zone of the dual space is itself maximized for a regular hexagonal lattice. Such a max-min optimization of $R_{b0}(\boldsymbol{k})$ was shown in Proposition 5.3 to characterize the optimal stability threshold for the inhibitor diffusivity. It would also be interesting to extend our linear stability theory to allow for a honeycomb-type lattice arrangement of localized spots, and to determine whether such a lattice offers a larger stability threshold for D than does a regular hexagonal lattice. Finally, it would be worthwhile to analyze the small eigenvalues of $\mathcal{O}(\epsilon^2)$ in the linearization and identify the corresponding optimal Bravais lattice for such weak translational instabilities of the spot pattern. For this class of small eigenvalues, it would be interesting to determine whether the instability threshold value of D is due to long-wavelength perturbations as was found for the case of conventional Turing-type periodic patterns (cf. [5], [6]). In our extended NLEP analysis in §5 of $\mathcal{O}(1)$ time-scale spot amplitude instabilities, long-wavelength perturbations do not set the stability threshold (see Fig. 6). To analyze such weak translational instabilities of spot patterns on a Bravais lattice, we would require an explicit representation of a new Bloch-Green's function having a dipole singularity.

A The Scaling Limit for the Brusselator Model

The Brusselator RD model, formulated in [21], is a well-known prototypical RD system that has been used to analyze various aspects spatio-temporal pattern formation. In a 2-D bounded domain Ω, and in the singularly perturbed limit $\epsilon_0\ll 1$, it has the form

$$V_\sigma=\epsilon_0^2\Delta V+E-(B+1)V+UV^2\,,\qquad U_\sigma=\mathcal{D}\Delta U+BV-UV^2\,;\qquad \sigma>0\,,\quad \mathbf{x}\in\Omega\,, \tag{A.1}$$

where B, D, and E are positive constants, and $\partial_n U=\partial_n V=0$ on $\partial\Omega$. Since localized spot patterns in 2-D occur when $E=\mathcal{O}(\epsilon_0)$ (cf. [22], [24]), we introduce the $\mathcal{O}(1)$ constant E_0 by $E=\epsilon_0 E_0$, and then define the new variables $V=E_0 v/\epsilon_0$, $U=\epsilon_0 B u/E_0$, and $\sigma=t/(B+1)$. In terms of these new variables, (A.1) becomes (1.1), where the positive $\mathcal{O}(1)$ parameters in (1.1) are

$$f\equiv\frac{B}{B+1}<1\,,\qquad \tau\equiv\frac{(B+1)^2}{E_0^2}\,,\qquad D\equiv\frac{\mathcal{D}(B+1)}{E_0^2}\,,\qquad \epsilon\equiv\frac{\epsilon_0}{\sqrt{B+1}}\,. \tag{A.2}$$

Acknowledgments

Michael J. Ward and Juncheng Wei were supported by NSERC Discovery grants. Justin Tzou was partially supported by a PIMS CRG Postdoctoral Fellowship. Yifan Chang was supported by a graduate research stipend while at UBC.

References

[1] M. Abramowitz, I. Stegun, *Handbook of mathematical functions*, 9th edition, New York, NY, Dover Publications.

[2] Y. A. Astrov, H. G. Purwins, *Spontaneous division of dissipative solitons in a planar gas-discharge system with high ohmic electrode*, Phys. Lett. A, **358**(5-6), (2006), pp. 404–408.

[3] D. Avitabile, V. Brena-Medina, M. J. Ward, *Spot dynamics in a plant root hair initiation model*, to appear, SIAM J. Appl. Math., (2016), (28 pages).

[4] G. Beylkin, C. Kurcz, L. Monzón, *Fast algorithms for Helmholtz Green's functions*, Proc. R. Soc. A, **464**, (2008), pp. 3301-3326.

[5] T. K. Callahan, E. Knobloch, *Symmetry-breaking bifurcations on cubic lattices*, Nonlinearity, **10**(5), (1997), pp. 1179-1216.

[6] T. K. Callahan, E. Knobloch, *Long-wavelength instabilities of three dimensional patterns*, Phys. Rev. E., **64**(3), 036214, (2001).

[7] W. Chen, M. J. Ward, *The stability and dynamics of localized spot patterns in the two-dimensional Gray-Scott model*, SIAM J. Appl. Dyn. Sys., **10**(2), (2011), pp. 582–666.

[8] P. W. Davis, P. Blanchedeau, E. Dullos and P. De Kepper, *Dividing blobs, chemical flowers, and patterned islands in a reaction-diffusion system*, J. Phys. Chem. A, **102**(43), (1998), pp. 8236–8244.

[9] FlexPDE6, *PDE Solutions Inc. URL http://www.pdesolutions.com*

[10] D. Iron, J. Rumsey, M. J. Ward, J. Wei, *Logarithmic expansions and the stability of periodic patterns of localized spots for reaction-diffusion systems*, J. Nonlinear Science, **24**(5), (2014), pp. 857–912.

[11] T. Kolokolnikov, M. J. Ward, J. Wei, *Spot self-replication and dynamics for the Schnakenberg model in a two-dimensional domain*, J. Nonlinear Sci., **19**(1), (2009), pp. 1–56.

[12] T. Kolokolnikov, M. Titcombe, M. J. Ward, *Optimizing the fundamental Neumann eigenvalue for the Laplacian in a domain with small traps*, Europ. J. Appl. Math., **16**(2), (2005), pp. 161–200.

[13] T. Kolokonikov, M. J. Ward, J. Wei, *The stability of hot-spot patterns for a reaction-diffusion system of urban crime*, DCDS-B, **19**(5), (2014), pp. 1373–1410.

[14] E. Knobloch, *Spatial localization in dissipative systems*, Ann. Rev. Cond. Mat. Phys., **6**, (2015), pp. 325–359.

[15] M. C. Kropinski, B. D. Quaife, *Fast integral equation methods for the modified Helmholtz equation*, J. Comp. Phys., **230**(2), (2011), pp. 425–434.

[16] K. J. Lee, W. D. McCormick, J. E. Pearson, H. L. Swinney, *Experimental observation of self-replicating spots in a reaction-diffusion system*, Nature, **369**, (1994), pp. 215-218.

[17] C. Muratov, V. V. Osipov, *Spike autosolitons and pattern formation scenarios in the two-dimensional Gray-Scott model*, Eur. Phys. J. B. **22**, (2001), pp. 213–221.

[18] C. Muratov, V. V. Osipov, *Stability of static spike autosolitons in the Gray-Scott model*, SIAM J. Appl. Math., **62**(5), (2002), pp. 1463–1487.

[19] Y. Nishiura, *Far-from equilibrium dynamics, translations of mathematical monographs*, Vol. **209**, (2002), AMS Publications, Providence, Rhode Island.

[20] J. E. Pearson, *Complex patterns in a simple system*, Science, **216**, (1993), pp. 189–192.

[21] I. Prigogine, R. Lefever, *Symmetry breaking instabilities in dissipative systems. II*, J. Chem. Physics, **48**, (1968), pp. 1695.

[22] I. Rozada, S. Ruuth, M. J. Ward, *The stability of localized spot patterns for the Brusselator on the sphere*, SIAM J. Appl. Dyn. Sys., **13**(1), (2014), pp. 564–627.

[23] L. Sewalt, A. Doelman, *Spatially periodic multi-pulse patterns in a generalized Klausmeier-Gray-Scott model*, to appear, SIAM J. Appl. Dyn. Sys., (2017)

[24] P. Trinh, M. J. Ward, *The dynamics of localized spot patterns for reaction-diffusion systems on the sphere*, Nonlinearity, **29**(3), (2016), pp. 766–806.

[25] J. Tzou, S. Xie, T. Kolokolnikov, M. J. Ward, *The stability and slow dynamics of localized spot patterns for the 3-D Schnakenberg reaction-diffusion model*, SIAM J. Appl. Dyn. Sys. **16**(1), (2017), pp. 294–336.

[26] J. Tzou, M. J. Ward, *The stability and slow dynamics of spot patterns in the 2D Brusselator model: the effect of open systems and heterogeneities*, under revision, Physica D, (2017), (38 pages).

[27] J. Tzou, M. J. Ward, J. Wei, *Anomalous scaling of Hopf bifurcation thresholds for the stability of localized spot patterns for reaction-diffusion systems in 2-D*, submitted, SIAM J. Appl. Dyn. Sys., (2017), (33 pages).

[28] A. Turing, *The chemical basis of morphogenesis*, Phil. Trans. Roy. Soc. B, **327**, (1952), pp. 37–72.

[29] V. K. Vanag, I. R. Epstein, *Localized patterns in reaction-diffusion systems*, Chaos **17**(3), 037110, (2007).

[30] M. J. Ward, *Spots, traps, and patches: Asymptotic analysis of localized solutions to some linear and nonlinear diffusive systems*, invited survey article, submitted, Nonlinearity, (2017), (35 pages).

[31] M. J. Ward, J. Wei, *Hopf bifurcation and oscillatory instabilities of spike solutions for the one-dimensional Gierer-Meinhardt model*, J. Nonlinear Sci. **13**(2), (2003), pp. 209–264.

[32] J. Wei, M. Winter, *Spikes for the two-dimensional Gierer-Meinhardt system: the weak coupling case*, J. Nonlinear Sci., **11**(6), (2001), pp. 415–458.

[33] J. Wei, M. Winter, *Existence and stability of multiple spot solutions for the Gray-Scott model in* $\mathbb{R}^2$, Physica D, **176**(3-4), (2003), pp. 147-180.

[34] J. Wei, M. Winter, *Stationary multiple spots for reaction-diffusion systems*, J. Math. Biol., **57**(1), (2008), pp. 53–89.

[35] J. Wei, *Existence and stability of spikes for the Gierer-Meinhardt system*, book chapter in: *Handbook of Differential Equations, Stationary Partial Differential Equations*, Vol. 5 (M. Chipot ed.), Elsevier, (2008), pp. 489–581.

[36] J. Wei, M. Winter, *Mathematical aspects of pattern formation in biological systems*, Applied Mathematical Science Series, Vol. 189, Springer, (2014).

[37] S. Xie, T. Kolokolnikov, *Moving and jumping spot in a two dimensional reaction-diffusion model*, to appear, Nonlinearity, (2018), (21 pages).